Inorg. Chem. **2007**, *46*, 6353–6372

Mechanism of Cis-Dihydroxylation and Epoxidation of Alkenes by Highly H_2O_2 Efficient Dinuclear Manganese Catalysts

Johannes W. de Boer,[†] Wesley R. Browne,[†] Jelle Brinksma,[†] Paul L. Alsters,[‡] Ronald Hage,[§] and Ben L. Feringa*[,†]

Stratingh Institute for Chemistry, University of Groningen, Nijenborgh 4, 9747 AG Groningen, The Netherlands, Advanced Synthesis, Catalysis and Development, DSM Pharma Products, PO Box 18, 6160 MD Geleen, The Netherlands, and Unilever R&D Vlaardingen, PO Box 114, 3130 AC Vlaardingen, The Netherlands

Received February 26, 2007

In the presence of carboxylic acids the complex $[Mn^{IV}_2(\mu\text{-}O)_3(tmtacn)_2]^{2+}$ (**1**, where tmtacn = *N*,*N*′,*N*″-trimethyl-1,4,7-triazacyclononane) is shown to be highly efficient in catalyzing the oxidation of alkenes to the corresponding *cis*-diol and epoxide with H_2O_2 as terminal oxidant. The selectivity of the catalytic system with respect to (w.r.t.) either *cis*-dihydroxylation or epoxidation of alkenes is shown to be dependent on the carboxylic acid employed. High turnover numbers (t.o.n. > 2000) can be achieved especially w.r.t. *cis*-dihydroxylation for which the use of 2,6-dichlorobenzoic acid allows for the highest t.o.n. reported thus far for *cis*-dihydroxylation of alkenes catalyzed by a first-row transition metal and high efficiency w.r.t. the terminal oxidant (H_2O_2). The high activity and selectivity is due to the in situ formation of bis(μ-carboxylato)-bridged dinuclear manganese(III) complexes. Tuning of the activity of the catalyst by variation in the carboxylate ligands is dependent on both the electron-withdrawing nature of the ligand and on steric effects. By contrast, the *cis*-diol/epoxide selectivity is dominated by steric factors. The role of solvent, catalyst oxidation state, H_2O, and carboxylic acid concentration and the nature of the carboxylic acid employed on both the activity and the selectivity of the catalysis are explored together with speciation analysis and isotope labeling studies. The results confirm that the complexes of the type $[Mn_2(\mu\text{-}O)(\mu\text{-}R\text{-}CO_2)_2(tmtacn)_2]^{2+}$, which show remarkable redox and solvent-dependent coordination chemistry, are the resting state of the catalytic system and that they retain a dinuclear structure throughout the catalytic cycle. The mechanistic understanding obtained from these studies holds considerable implications for both homogeneous manganese oxidation catalysis and in understanding related biological systems such as dinuclear catalase and arginase enzymes.

Introduction

Oxidative transformations[1] and especially cis-dihydroxylation and epoxidation of alkenes are key chemical processes in biology,[2] synthetic organic chemistry, and the chemical industry.[3,4,5] In recent years, considerable advances have been made in the development of atom-efficient and environmentally friendly catalytic methods employing H_2O_2,[3] most notably in the use of Mn^{II} salts[6] and complexes[7] and Fe^{II} complexes[8] in the catalytic epoxidation of alkenes. Among the many oxidative transformations that are of synthetic interest, first-row transition metal catalyzed cis-dihydroxylation of alkenes[4] remains one of the most challenging. The reports by De Vos and co-workers on heterogenized Mn−tmtacn[9] (where tmtacn = *N*,*N*′,*N*″-trimethyl-1,4,7-triazacy-

* To whom correspondence should be addressed. E-mail: b.l.feringa@rug.nl.
† University of Groningen.
‡ DSM Pharma Products.
§ Unilever R&D Vlaardingen.

(1) Backvall, J.-E., Ed. *Modern Oxidation Methods*; Wiley-VCH: Weinheim, Germany, 2004.
(2) Wu, A. J.; Penner-Hahn, J. E.; Pecoraro, V. L. *Chem. Rev.* **2004**, *104*, 903−938.
(3) (a) Lane, B. S.; Burgess, K. *Chem. Rev.* **2003**, *103*, 2457−2473. (b) Sheldon, R. A.; Kochi, J. K. *Metal-Catalyzed Oxidations of Organic Compounds*; Academic Press: New York, 1981. (c) Brinksma, J.; de Boer, J. W.; Hage, R.; Feringa, B. L. In *Modern Oxidation Methods*; Bäckvall, J.-E., Ed.; Wiley-VCH: Weinheim, Germany, 2004; Chapter 10, pp 295−326. (d) Noyori, R; Aoki, M.; Sato, K. *Chem. Commun.* **2003**, 1977−1986. (e) Katsuki, T. *Chem. Soc. Rev.* **2004**, *33*, 437−444. (f) Punniyamurthy, T.; Velusamy, S.; Iqbal, J. *Chem. Rev.* **2005**, *105*, 2329−2364.
(4) Kolb, H. C.; Van Nieuwenhze, M. S.; Sharpless, K. B. *Chem. Rev.* **1994**, *94*, 2483−2547.

10.1021/ic7003613 CCC: $37.00
Published on Web 07/03/2007

Scheme 1. Cis-Dihydroxylation and Epoxidation of Alkenes by **1**

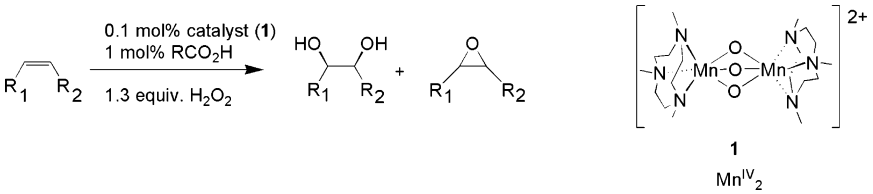

clononane) and Que and co-workers with Fe^{II} pyridyl-amine-based complexes[8] and our own recent report on the use of the oxidation catalyst $[Mn^{IV}_2O_3(tmtacn)_2]^{2+}$ (**1**, Scheme 1),[10] in the presence of carboxylic acids,[11] have demonstrated the potential of first-row transition metals toward cis-dihydroxylation of alkenes.

Manganese complexes based on the ligand tmtacn, such as **1** (Scheme 1), were developed in the late 1980s and -90s as functional models for bioinorganic manganese systems,[10,12] in particular, dinuclear manganese based catalase[2,13,14] enzymes and the water-splitting component of photosystem II (PSII).[15] The catalytic properties of these complexes toward oxidative transformations with H_2O_2 in both aqueous[16] and nonaqueous[17] media have, however, made the tmtacn family of complexes the focus of considerable interest for a whole range of oxidative transformations including textile stain bleaching,[18] benzyl alcohol oxidation,[17c] C−H bond activation,[17f] sulfoxidation,[19] and cis-dihydroxylation and epoxidation of alkenes.[11,16,17]

In our recent communication,[11] we reported that **1** can engage in the atom-efficient cis-dihydroxylation of alkenes with high turnover numbers when combined with electron deficient carboxylic acids (Figure 1). We demonstrated that the use of carboxylic acids at cocatalytic levels is effective in suppressing the inherent catalase activity of **1**[10] and allows for the tuning of the catalyst's selectivity toward either cis-dihydroxylation or epoxidation. Preliminary kinetic and spectroscopic measurements[11] indicated that control over the outcome of the reaction toward cis-dihydroxylation or epoxidation presumably arises from the in situ formation of carboxylato-bridged dinuclear complexes, e.g., complex **2a** $\{[Mn^{III}_2(\mu\text{-}O)(\mu\text{-}CCl_3CO_2)_2(tmtacn)_2]^{2+}\}$, during catalysis (Figure 1).

In this paper a full account of the structural and mechanistic features as well as the parameters that govern the activity and selectivity of the catalysis of this exceptionally H_2O_2 efficient catalytic system is provided. The role of **2a** in the catalysis and the importance of the formation of the μ-carboxylato-bridged dinuclear manganese(II) complex **2c** (in which the μ-oxido bridge is replaced by two labile OH/H_2O ligands) and its Mn^{III}_2 analog (**2d**) is addressed (Figure 1). We demonstrate that the dominant species present under catalytic conditions are dinuclear bis(μ-carboxylato)-bridged complexes (e.g., **2a**,**d**) and that the reaction of these complexes with H_2O and H_2O_2 is rate limiting. Furthermore, we show that in addition to consideration of the molecular catalyst, bulk solvent conditions must be taken into account in understanding the behavior of the reaction system overall in terms of reactivity and selectivity.

Experimental Section

All reagents were of commercial grade (Aldrich, Acros, Fluka) and were used as received unless stated otherwise. Dihydrogen

(5) (a) Nelson, D. W.; Gypser, A.; Ho, P. T.; Kolb, H. C.; Kondo, T.; Kwong, H.-L.; McGrath, D. V.; Rubin, A. E.; Norrby, P.-O.; Gable, K. P.; Sharpless, K. B. *J. Am. Chem. Soc.* **1997**, *119*, 1840−1858. (b) Katsuki, T.; Sharpless, K. B. *J. Am. Chem. Soc. 1980*, **102**, 5974−5976. (c) Sato, K.; Aoki, M.; Ogawa, M.; Hashimoto, T.; Noyori, R. *J. Org. Chem.* **1996**, *61*, 8310−8311. (d) Herrmann, W. A.; Fischer, R. W.; Marz, D. W. *Angew. Chem., Int. Ed. Engl.* **1991**, *30*, 1638−1641.

(6) Lane, B. S.; Vogt, M.; DeRose, V. J.; Burgess, K. *J. Am Chem. Soc.* **2002**, *124*, 11946−11954.

(7) (a) McGarrigle, E. M.; Gilheany, D. G. *Chem. Rev.* **2005**, *105*, 1563−1602. (b) Katsuki, T. *Coord. Chem. Rev.* **1995**, *140*, 189−214.

(8) (a) Fujita, M.; Costas, M.; Que, L., Jr. *J. Am. Chem. Soc.* **2003**, *125*, 9912−9913. (b) Chen, K.; Costas, M.; Kim, J.; Tipton, A. K.; Que, L., Jr. *J. Am. Chem. Soc.* **2002**, *124*, 3026−3035. (c) Ryu, J. Y.; Kim, J.; Costas, M.; Chen, K.; Nam, W.; Que, L., Jr. *Chem. Commun.* **2002**, 1288−1289. (d) Mas-Balleste, R.; Costas, M.; van den Berg, T.; Que, L., Jr. *Chem.*−Eur. J. **2006**, *12*, 7489−7500. (e) Oldenburg, P. D.; Que, L., Jr. *Catal. Today* **2006**, *117*, 15−21. (f) Bukowski, M. R.; Comba, P.; Lienke, A.; Limberg, C.; Lopez, de Laorden, C.; Mas-Balleste, R.; Merz, M.; Que, L., Jr. *Angew. Chem.* **2006**, *45*, 3446−3449. (g) Oldenburg, P. D.; Ke, C.-Y.; Tipton, A. A.; Shteinman, A. A.; Que., L., Jr. *Angew. Chem., Int. Ed.* **2006**, *45*, 7975−7978. (h) Oldenburg, P. D.; Shteinman, A. A.; Que, L., Jr. *J. Am. Chem. Soc.* **2005**, *127*, 15672−15673.

(9) De Vos, D. E.; De Wildeman, S.; Sels, B. F.; Grobet, P. J.; Jacobs, P. A. *Angew. Chem., Int. Ed.* **1999**, *38*, 980−983.

(10) (a) Wieghardt, K.; Bossek, U.; Nuber, B.; Weiss, J.; Bonvoisin, J.; Corbella, M.; Vitols, S. E.; Girerd, J. J. *J. Am. Chem. Soc.* **1988**, *110*, 7398−7411. (b) Darovsky, A.; Kezerashvili, V.; Coppens, P.; Weyhermuller, T.; Hummel, H.; Wieghardt, K. *Inorg. Chem.* **1996**, *35*, 6916−6917. (c) Hage, R.; Krijnen, B.; Warnaar, J. B.; Hartl, F.; Stufkens, D. J.; Snoeck, T. L. *Inorg. Chem.* **1995**, *34*, 4973−4978. (d) Bossek, U.; Weyhermuller, T.; Wieghardt, K.; Nuber, B.; Weiss, J. *J. Am. Chem. Soc.* **1990**, *112*, 6387−6388.

(11) de Boer, J. W.; Brinksma, J.; Browne, W. R.; Meetsma, A.; Alsters, P. L.; Hage, R.; Feringa, B. L. *J. Am. Chem. Soc.*, **2005**, *127*, 7990−7991.

(12) de Boer, J. W.; Browne, W. R.; Feringa, B. L.; Hage, R. *C. R. Chimie* **2007**, *10*, 341−354.

(13) (a) Pecoraro, V. L.; Baldwin, M. J.; Gelasco, A. *Chem. Rev.* **1994**, *94*, 807−826. (b) Jackson, T. A.; Brunold, T. C. *Acc. Chem. Res.* **2004**, *37*, 461−470. (c) Boelrijk, A. E. M.; Khangulov, S. V.; Dismukes, G. C. *Inorg. Chem.* **2000**, *39*, 3009−3019. (d) Boelrijk, A. E. M.; Dismukes, G. C. *Inorg. Chem.* **2000**, *39*, 3020−3028.

(14) Kanyo, Z. F.; Scolnick, L. R.; Ash, D. E.; Christianson, D. W. *Nature* **1996**, *383*, 554−557.

(15) (a) Sauer, K. *Acc. Chem. Res.* **1980**, *13*, 249−256. (b) Mukhopadhyay, S.; Mandal, S. K.; Bhaduri, S.; Armstrong, W. H. *Chem. Rev.* **2004**, *104*, 3981−4026. (c) Yachandra, V. K.; Sauer, K.; Klein, M. P. *Chem. Rev.* **1996**, *96*, 2927−2950. (d) Yagi, M.; Kaneko, M. *Chem. Rev.* **2001**, *101*, 21−36. (e) Sun, L.; Hammarström, L.; Åkermark, B.; Styring, S. *Chem. Soc. Rev.* **2001**, *1*, 36−49. (f) Yano, J.; Sauer, K.; Girerd, J.-J.; Yachandra, V. K. *J. Am. Chem. Soc.* **2004**, *126*, 7486−7495. (g) Yachandra, V. K.; DeRose, V. J.; Latimer, M. J.; Mukerji, I.; Sauer, K.; Klein, M. P. *Science* **1993**, *260*, 675−679. (h) Baranov, S. V.; Tyryshkin, A. M.; Katz, D.; Dismukes, G. C.; Ananyev, G. M.; Klimov, V. V. *Biochemistry* **2004**, *43*, 2070−2079. (i) Ruttinger, W.; Dismukes, G. C. *Chem. Rev.* **1997**, *97*, 1−24. (j) McEvoy, J. P.; Brudvig, G. W. *Chem. Rev.* **2006**, *106*, 4455−4483.

(16) Hage, R.; Iburg, J. E.; Kerschner, J.; Koek, J. H.; Lempers, E. L. M.; Martens, R. J.; Racherla, U. S.; Russell, S. W.; Swarthoff, T.; van Vliet, M. R. P.; Warnaar, J. B.; van der Wolf, L.; Krijnen, B. *Nature* **1994**, *369*, 637−639.

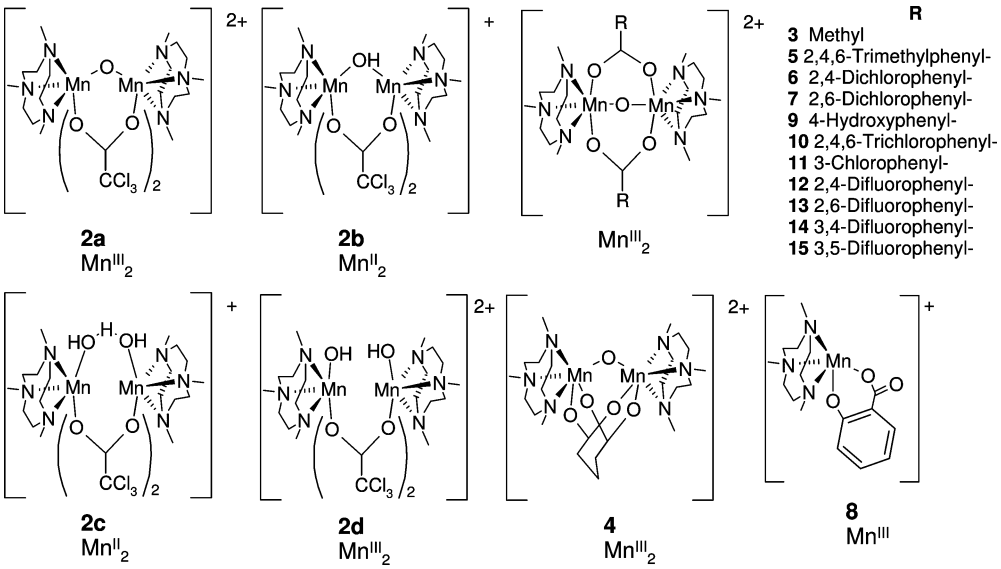

Figure 1. Complexes described in the text. Complexes **2a**,[11] **2b**,[11] and **3**[10a] have been characterized structurally. For complexes **2c**,**d** and **5**−**15**, see the Supporting Information.

peroxide used: 50% v/w (Acros) or 30% v/v (Merck, medicinal grade) solution in water. D_2O_2 (Icon Isotopes): 30% solution in D_2O, 99 atom % D. D_2O (Aldrich): 99.9 at. % D. $H_2{}^{18}O_2$ (Icon Isotopes): 2% solution in $H_2{}^{16}O$, 90 at. % ^{18}O. $H_2{}^{18}O$ (Icon Isotopes): 97 at. % ^{18}O. *cis*-2,3-Epoxyheptane, *trans*-2,3-epoxyheptane, *threo*-2,3-heptanediol, and *erythro*-2,3-heptanediol were prepared by literature procedures[20] and characterized by ^1H and ^{13}C NMR spectroscopy and HRMS. The synthesis and characterization of complexes **1**,[10a] **2a**,[11] **2b**,[11] and **3**[10a] were reported previously. Full synthetic procedures and analytical, spectroscopic, and electrochemical data for complexes **2c** and **4**−**15** are provided as Supporting Information (SI).

Caution! Perchlorate salts of metal complexes incorporating organic ligands are potentially explosive. These compounds should be prepared in small quantities and handled with suitable protective safe guards.

Caution! The removal of water from aqueous H_2O_2 solutions by mixing with organic solvents followed by drying over magnesium sulfate is hazardous and should be performed only in small quantities and handled with suitable protective safe guards.

Definition of t.o.n., RC, and Mass Balance. Turnover number (t.o.n.): mol of product/mol of catalyst. RC (retention of configuration) = 100% × $(A - B)/(A + B)$, where A = yield of product with retention of configuration and B = yield of epimer.[21] Mass balance (%) = unreacted alkene (%) + [*cis*-diol and epoxide products (%)]. Deviation from a mass balance of 100% indicates loss through further oxidation of the *cis*-diol formed initially and/or the occurrence of competing oxidation pathways other than *cis*-dihydroxylation and epoxidation.[11]

Physical Measurements. ^1H NMR spectra (400.0 MHz) and ^{19}F NMR (121.5 MHz) spectra were recorded on a Varian Mercury Plus. Chemical shifts are denoted relative to the solvent residual peak (^1H NMR spectra CD_3CN: 1.94 ppm) or PF_6^- (^{19}F NMR spectra PF_6^-: 74.8, 243 Hz). Elemental analyses were performed with a Foss-Heraeus CHN-O-Rapid or a EuroVector Euro EA elemental analyzer. Electrochemical measurements were carried out on a model 630B Electrochemical Workstation (CH Instruments). Analyte concentrations were typically 0.5−1.0 mM in anhydrous acetonitrile containing 0.1 M tetrabutylammonium hexafluorophosphate [(TBA)PF_6]. Unless stated otherwise, a Teflon-shrouded glassy carbon working electrode (CH Instruments), a Pt wire auxiliary electrode, and an SCE reference electrode were employed (calibrated externally using 0.1 mM solutions of ferrocene in 0.1 M (TBA)PF_6/CH_3CN). Cyclic voltammograms were obtained at sweep rates between 1 mV s^{-1} and 10 V s^{-1}. For reversible processes, the half-wave potential values are reported. Redox potentials are reported ±10 mV. EPR spectra (X-band, 9.46 GHz) were recorded on a Bruker ECS106 instrument in liquid nitrogen (77 K). Samples for measurement were transferred from the reaction solution (250 μL) to an EPR tube, which was frozen to 77 K immediately.

UV−vis spectra were recorded on a Hewlett-Packard 8453 spectrophotometer using either 2 or 10 mm path length quartz cuvettes. Electrospray ionization mass spectra were recorded on a Triple Quadrupole LC/MS/MS mass spectrometer (API 3000, Perkin-Elmer Sciex Instruments). A sample (2 μL) was taken from the reaction mixture at the indicated times (vide infra) and was diluted in CH_3CN (1 mL) before injection in the mass spectrometer (via syringe pump). Mass spectra were measured in positive mode

(17) (a) Berkessel, A.; Sklorz, C. A. *Tetrahedron Lett.* **1999**, *40*, 7965−7968. (b) De Vos, D. E.; Bein, T. *Chem. Commun.* **1996**, 917−918. (c) Zondervan, C.; Hage, R.; Feringa, B. L. *Chem. Commun.* **1997**, 419−420. (d) De Vos, D. E.; Sels, B. F.; Reynaers, M.; Subba Rao, Y. V.; Jacobs, P. A. *Tetrahedron Lett.* **1998**, *39*, 3221−3224. (e) Woitiski, C. B.; Kozlov, Y. N.; Mandelli, D.; Nizova, G. V.; Schuchardt, U.; Shul'pin, G. B. *J. Mol. Catal., A* **2004**, *222*, 103−119. (f) Bolm, C.; Meyer, N.; Raabe, G.; Weyhermuller, T.; Bothe, E. *Chem. Commun.* **2000**, 2435−2436. (g) Chin Quee-Smith, V.; DelPizzo, L.; Jureller, S. H.; Kerschner, J. L.; Hage. R. *Inorg. Chem.* **1996**, *35*, 6461−6465. (h) De Vos, D. E.; Bein, T. *Chem. Commun.* **1996**, 917−918. (i) Gilbert, B. C.; Smith, J. R. L.; Payeras, A. M.; Oakes, J.; Pons i Prats, R. *J. Mol. Catal., A: Chem.* **2004**, *219*, 265−272. (j) Ryu, J. Y.; Kim, S. O.; Nam, W.; Heo, S.; Kim, J. *Bull. Korean Chem. Soc.* **2003**, *24*, 1835−1837. (k) Lindsay Smith, J. R.; Gilbert, B. C.; Mairata i Payeras, A.; Murray, J.; Lowdon, T. R.; Oakes, J.; Pons i Prats, R.; Walton, P. H. *J. Mol. Catal., A: Chem.* **2006**, *251*, 114−122 and references cited herein. (l) Brinksma, J.; Schmieder, L.; van Vliet, G.; Boaron, R.; Hage, R.; De Vos, D. E.; Alsters, P. L.; Feringa, B. L. *Tetrahedron Lett.* **2002**, *43*, 2619−2622.
(18) Hage, R.; Lienke, A. *Angew. Chem., Int. Ed.* **2006**, *45*, 202−222.
(19) Barker, J. E.; Ren, T. *Tetrahedron Lett.* **2004**, *45*, 4681−4683.
(20) (a) Kroutil, W.; Mischitz, M.; Faber, K. *J. Chem. Soc., Perkin Trans. 1* **1997**, 3629−3636. (b) Chiappe, C.; Cordoni, A.; Lo Moro, G.; Palese, C. D. *Tetrahedron: Asymmetry* **1998**, *9*, 341−350.
(21) Chen, K.; Que, L., Jr. *J. Am. Chem. Soc.* **2001**, *123*, 6327−6337.

and in the range *m*/*z* 100−1500. Ion-spray voltage: 5200 V. Orifice: 15 V. Ring: 150 V. Q_0: −10 V.

Ligand exchange of the μ-oxido bridge of $[Mn^{III}_2(\mu\text{-}^{16}O)(\mu\text{-}CCl_3CO_2)_2(tmtacn)]^{2+}$, $[Mn^{III}_2(\mu\text{-}^{16}O)(\mu\text{-}CH_3CO_2)_2(tmtacn)]^{2+}$, and $[Mn^{III}_2(\mu\text{-}^{16}O)(\mu\text{-}2,6\text{-dichlorobenzoate})_2(tmtacn)]^{2+}$ was monitored by ESI-MS. Measurements were performed at concentrations used in catalytic reactions (i.e., 1 mM in complex), and samples were injected directly into the ESI-MS using a syringe pump and PEEKsil tubing (normal probe and without dilution). API-365 settings: orifice, +15 V; ring, +150 V; Q_0, −5 V. For kinetic measurements only, a small portion of the spectrum was recorded to minimize measuring time between each subsequent data point while monitoring the $[Mn^{III}_2(\mu\text{-}O)(\mu\text{-}RCO_2)_2(tmtacn)]^{2+}$ ion. The presence of cyclooctene (1 M) and of carboxylic acid (1.0 mol %) did not result in significant interference of the mass spectra of **1** or **2a**,[22] and neither cyclooctene nor the *cis*-diol and epoxide products give rise to significant signals.[23] Importantly, even with 25 mol % CCl_3CO_2H, no free tmtacn ligand is observed, indicating that **1** is stable under these conditions prior to addition of H_2O_2.

Procedures Employed for Catalysis Studies. General Procedure A. The alkene (10 mmol), 1,2-dichlorobenzene (internal standard, 735 mg, 5.0 mmol), **1** (8.1 mg, 10 μmol), and cocatalyst (typically 0.10 mmol) in acetonitrile (10 mL) were cooled to 0 °C. H_2O_2 (0.74 mL, 13 mmol) was added via syringe pump over 6 h (0.12 mL/h). The reaction mixture was stirred at 0 °C for 1 h after the addition of H_2O_2 was completed, prior to sampling by GC.

General Procedure B (Catalyst Pretreatment with H_2O_2). H_2O_2 (30 μL, 0.53 mmol) was added to a mixture of 1,2-dichlorobenzene (735 mg, 5.0 mmol), **1** (8.1 mg, 10 μmol), and cocatalyst (e.g., trichloroacetic acid, 0.10 mmol) in acetonitrile (7 mL) at room temperature. The mixture was stirred for 20 min, after which the alkene (10 mmol) was added together with acetonitrile (3 mL) and the mixture was cooled to 0 °C. H_2O_2 (0.71 mL, 12.5 mmol) was added via syringe pump (0.12 mL/h). The reaction mixture was stirred at 0 °C for 1 h after the addition of H_2O_2 was completed, prior to sampling by GC.

GC analyses were performed on an Agilent 6890 gas chromatograph equipped with a HP-1 dimethyl polysiloxane column (30 m × 0.25 mm × 0.25 μm). Peak identification and calibration were performed using independent samples (either purchased from a commercial supplier or synthesized independently[11]). Conversion and turnover numbers were determined in duplo by employing 1,2-dichlorobenzene as internal standard. All values are ±10%.

^{18}O-Labeling. Samples at t = 60 min were analyzed by GC-MS using chemical ionization. GC: HP 6890 equipped with a HP-5 column (30 m × 0.32 mm × 0.25 μm). MS: JMS-600H using chemical ionization (reaction gas NH_3). The samples were analyzed by GC (HP-1 column) as described above also to determine t.o.n..

Results and Discussion

To understand the roles played by solvent, water, and carboxylic acid in determining the activity and selectivity of the catalytic system (vide infra), it is pertinent to first understand the redox and spectroscopic properties of the complexes that are, potentially, involved in the catalysis. In particular, a detailed study of the redox and solvent driven interconversion of complexes **2a**−**d**, their formation from **1**, and their behavior in the presence of H_2O_2 is central to understanding the catalytic system.

Synthesis and Characterization. The synthesis and structural characterization of complexes **1**,[10] **2a**,[11] **2b**,[11] and **3**[10] were reported previously. Complexes **4**−**7** and **9**−**15** (Figure 1) were prepared in good yield by ascorbic acid reduction of **1** in an aqueous solution containing the respective carboxylic acid (see SI for procedures and analytical and spectroscopic data). Overall, the Mn^{III}_2−bis-(μ-carboxylato) complexes exhibit solution chemistry similar to that of **3**;[10] however, the redox and electronic properties are affected significantly by the carboxylate ligand employed (see Table S1), with more electron-deficient carboxylates showing anodic shifts in the potential of all redox processes observed. The Mn^{II}_2 complex **2c** was prepared by reduction of **1** with 2 equiv of H_2NNH_2 in acetonitrile in the presence of 2 equiv of CCl_3CO_2H and isolated as a white powder (see SI for details).

The solid-state FTIR spectra of **2a**−**c** are shown in Figure S1. For **2a** the carboxylato bridge absorption is observed at 1659 cm^{-1}. The carboxylato absorptions of **2b**,**c** are very similar (∼1695 cm^{-1}). The absorptions assigned to the Cl_3COO^- moieties of **2a**,**b** are blue-shifted significantly (80−90 cm^{-1}) from the corresponding CH_3COO^--bridged complexes (1568 and 1615 cm^{-1},[10a] respectively).

In acetonitrile solution the carboxylato absorption band of **2a** at 1659 cm^{-1} is retained and its insensitivity to either CCl_3CO_2H or cyclooctene suggests that the bridging mode of the complex is the same as that determined for the solid state by X-ray crystallography[11] (Figure S2). Similarly both **2b**,**c** show a strong absorption at 1695 cm^{-1} in CH_3CN with 1 M cyclooctene present, identical with that observed in their solid-state spectra.

In the spectrum of **2a** an additional weak band is observed at 1735 cm^{-1}, which in the presence of CCl_3CO_2H shifts to 1720 cm^{-1} (Figure S3). Addition of CCl_3CO_2H (10 equiv) to a solution of **2b** in CH_3CN results in the disappearance of the absorption band at 1695 cm^{-1} and the appearance of a strong absorption band at 1720 cm^{-1}. Addition of D_2O results in the partial recovery of the absorption band at 1695 cm^{-1} (Figure S3). The carboxylato vibrations of the tris-(carboxylato)-bridged complex $[Mn^{II}_2(\mu\text{-}OAc)_3(tmtacn)_2]^+$, reported by Wieghardt et al.[10a] at 1636 cm^{-1}, are at higher energy than for the corresponding bis(carboxylato) $[Mn^{II}_2(\mu\text{-}OH)(\mu\text{-}OAc)_2(tmtacn)_2]^+$ (1615 cm^{-1}). This suggests that the absorption at 1720 cm^{-1} is due to the complex $[Mn^{II}_2(\mu$-

(22) Mass spectrometry has proven to be a powerful tool in the identification of species present in solution, not least for manganese systems. (a) Fenn, J. B.; Mann, M.; Meng, C. K.; Wong, S. F.; Whitehouse, C. M. *Mass Spectrom. Rev.* **1990**, *9*, 37−70. (b) Feichtinger, D.; Plattner, D. *Angew. Chem., Int. Ed. Engl.* **1997**, *36*, 1718−1719. (c) Feichtinger, D.; Plattner, D. *J. Chem. Soc., Perkin Trans.* **2000**, *2*, 1023−1028. (d) Gilbert, B. C.; Smith, J. R. L.; Mairata i Payeras, A.; Oakes, J. *Org. Biomol. Chem.* **2004**, *2*, 1176−1180. (e) Bortolini, O.; Conte, V. *Mass Spectrom. Rev.* **2006**, *25*, 724−740. However, caution should be exercised in its use as a mechanistic probe due to the possibility of experimental artifacts occurring such as reduction within the mass spectrometer itself and the presence of nondetectable neutral species. Indeed, the use of stabilizers in commercial grade chemicals, such as cyclooctene, highlights this point. One source of cyclooctene contained such a stabilizer, which provided signals in the MS experiments assignable to possible catalytic intermediates. The use of cyclooctene from a second source or triple distillation of the cyclooctene to remove the stabilizer while having no effect on other spectroscopic properties or catalysis did result in the elimination of these spurious signals.

(23) For **2a** at higher CCl_3CO_2H (10 mol %) concentrations, an additional signal at *m*/*z* 951 {assigned to $[Mn^{III}_2(O)(CCl_3CO_2)_2tmtacn_2](CCl_3CO_2)^+$} is observed.

Scheme 2. Summary of Redox Chemistry of **2a**−**d** in 0.1 M (TBA)PF_6/CH_3CN with 1 mol % CCl_3CO_2H

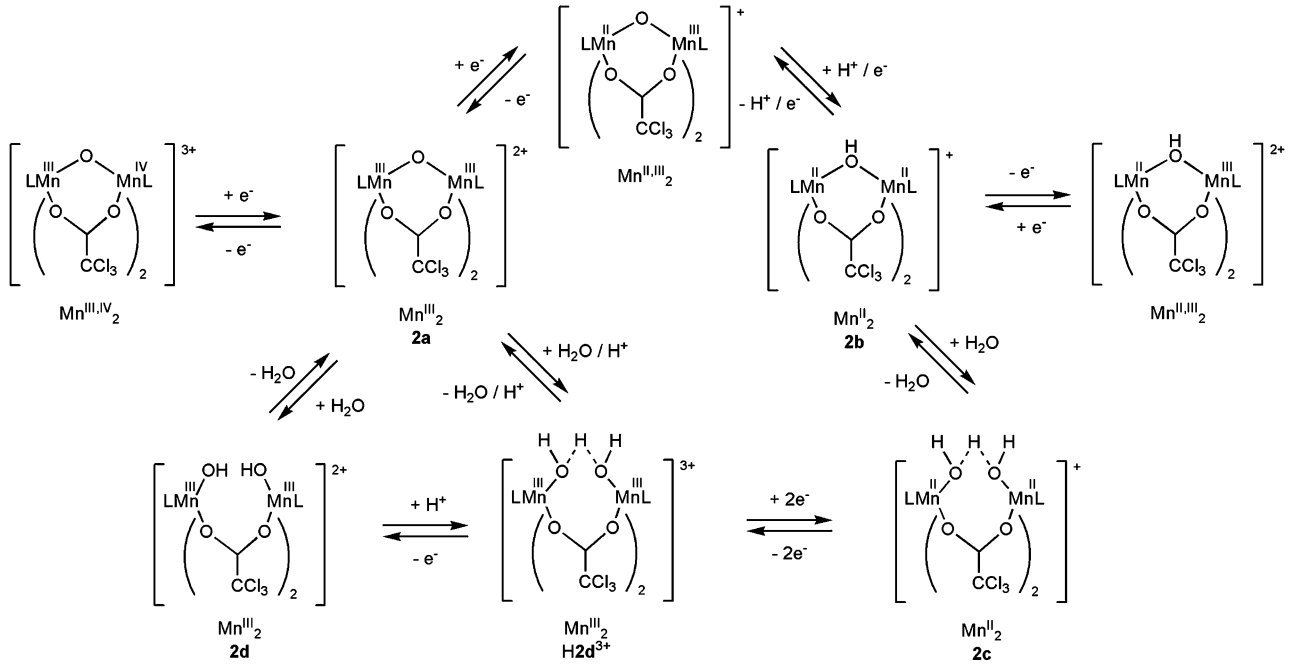

$CCl_3CO_2)_3(tmtacn)_2]^+$ (Scheme 3), formation of which is suppressed by addition of water.

Overall **2c** can be assigned as a bis(carboxylato)-bridged complex, which in the presence of excess CCl_3CO_2H is in equilibrium with a tris(carboxylato) complex, i.e., $[Mn^{II}_2(\mu\text{-}CCl_3CO_2)_3(tmtacn)_2]^+$. The nature of the third bridging unit of **2c**, however, is less clear. In the solid state, **2b** shows a very sharp absorption at 3620 cm^{-1}, assigned to the μ-O−H unit, which is present in the X-ray crystal structure. The O−H absorption band is equivalent to that of, for example, a dinuclear Zn^{II} complex reported by Meyer and Rutsch (ν = 3618 cm^{-1}).[24] The spectra of **2b**,**c** are strikingly similar in both the solid state and in acetonitrile solution; however, the sharp O−H absorption of **2b** is replaced by a broad set of three absorption bands in **2c** at 3593, 3433, and 3251 cm^{-1}. Although crystals of **2c** suitable for X-ray analysis have, thus far, not been obtained, we propose that complex **2c** contains a $\{Mn^{II}\text{-}(\mu\text{-}O_2H_3)\text{-}Mn^{II}\}$ structural motif (Figure 1) on the basis of ESI-MS, elemental analysis, and EPR and IR spectroscopy. The related Mn^{III}_2 complex **2d**, although stable in acetonitrile solution, was not isolated due to the equilibrium of this complex with complex **2a**. Hence, **2d** was characterized spectroscopically and electrochemically only (vide infra).

Electrochemical Properties of 2a−d. Both the Mn^{III}_2 complex **2a** and the Mn^{II}_2 complex **2b** have been characterized by X-ray crystallography.[11] The manganese centers are bridged by two carboxylato ligands and a μ-oxido or μ-hydroxido bridge, respectively (Figure 1). In acetonitrile solution both complexes are stable and show reversible one-electron redox processes (Figure 3a, Figure 4a, and Table S1; vide infra) in the absence of CCl_3CO_2H.

In the presence of 10 equiv of CCl_3CO_2H, a series of chemically irreversible redox processes are observed (Figure 4a). Although significant structural changes accompany some of the redox processes, overall "decomposition" of **2a** does not occur (Scheme 2 and Table 1).[25] The proton-coupled two-electron reduction of **2a** to form **2b** is followed, in the presence of a carboxylic acid, by opening of the μ-OH bridge to form the corresponding hydroxy−aqua complex, **2c**. The latter complex undergoes a two-electron oxidation to form $[Mn^{III}_2(\mu\text{-}O_2H_3)(\mu\text{-}CCl_3CO_2)_2(tmtacn)_2]^{3+}$ ($H\mathbf{2d}^{3+}$), which, depending upon the conditions employed, (i) shows a (quasi)-reversible two-electron reduction to form **2c** (0.94 V), (ii) undergoes deprotonation to form $[Mn^{III}_2(OH)_2(\mu\text{-}CCl_3CO_2)_2\text{-}(tmtacn)_2]^{2+}$ (**2d**), or (iii) undergoes a further chemical change: elimination of H_2O to re-form **2a**.

Table 1. Electronic and Redox Data for **2a**−**d** Complexes in CH_3CN/0.1 M (TBA)PF_6

compd	core	λ_{max}/nm	$E_{1/2}$ in V vs SCE ($E_{p,a} - E_{p,c}$/mV)
2a	$Mn^{III}_2(\mu\text{-}O)$	390, 494, 540	0.25 (80),[a] 1.40 (100)
2b	$Mn^{II}_2(\mu\text{-}OH)$	b	0.54 (110)
2c	$Mn^{II}_2(\mu\text{-}O_2H_3)$	b	0.99 (85, qr)
2d	$Mn^{III}_2(OH)_2$	300, 468	0.67 ($E_{p,c}$, irr)

[a] In CH_3CN/0.1 M (TBA)PF_6 with 10 mM CCl_3CO_2H, an irreversible 2 e^- reduction is observed at 0.29 ($E_{p,c}$). [b] Complex does not absorb in the visible or near-UV region.

(24) Meyer, F.; Rutsch, P. *Chem. Commun*. **1998**, 1037−1038.

(25) In the presence of electrolyte, **1** and **2a** show a moderate reduction in catalytic activity; however, overall the selectivity and reactivity is not affected significantly.

(26) The series of electron-transfer reactions which accompany the reduction of **1** to **2c** are expected to be outer sphere in nature on the basis of the equivalent reactions, which are observed electrochemically. If the reduction of **1** by H_2O_2 involves an outer-sphere double electron transfer, then it will result in the formation of O_2 [$Mn^{IV}_2 + 2e^- \rightarrow Mn^{III}_2$; $H_2O_2 \rightarrow O_2 + 2H^+ + 2e^-$]. However, it is also possible that inner-sphere single-electron-transfer processes are involved where H_2O_2 coordinates to **1**. This would complicate the description of the reaction: (i) $Mn^{IV}_2 + 1e^- \rightarrow Mn^{III}Mn^{IV}$ (often observed by EPR); ii) $2Mn^{III}Mn^{IV} \rightarrow Mn^{IV}_2 + Mn^{III}_2$ (disproportionation) or $Mn^{III}Mn^{IV} + e^- \rightarrow Mn^{III}_2$ and $H_2O_2 \rightarrow HO_2 + H^+ + 1e^-$ (and then $2HO_2 \rightarrow O_2 + H_2O_2$). The matter is complicated further by the fact that the conversion is autocatalytic, and hence, although H_2O_2 might be involved directly in the reaction initially, once the process of conversion of **1** has begun the involvement of species such as **2a**−**d** must be considered.

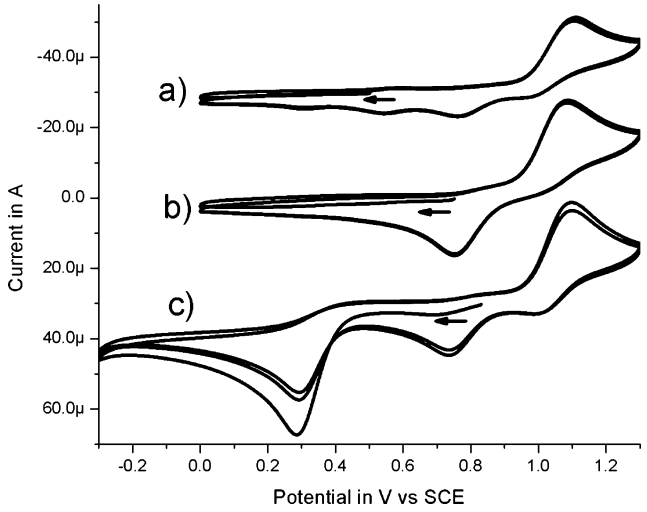

Figure 2. Cyclic voltammetry of **2c** (1 mM) in CH_3CN/0.1 M (TBA)PF_6 in the (a) absence and (b) presence of 10 mM CCl_3CO_2H and (c) **2a** with 10 mM CCl_3CO_2H. The current axes of (a) and (c) are offset by −30 and +30 μA, respectively, for clarity. Initial scan direction from the open circuit potential is cathodic in each case. Scan rate: 0.1 V s^{-1}.

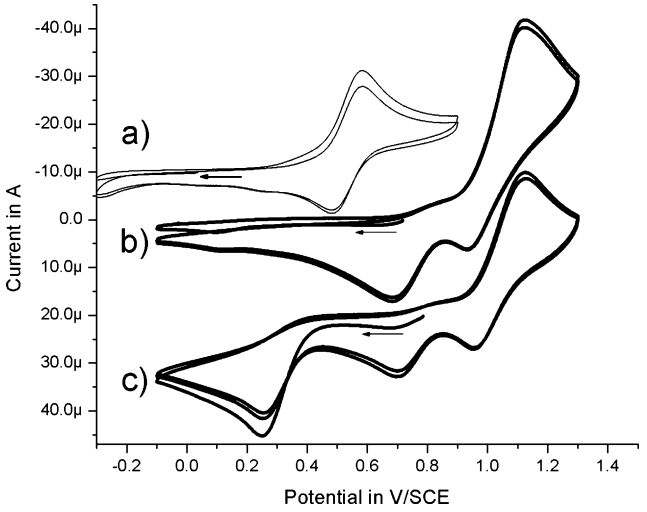

Figure 3. Cyclic voltammetry of **2b** in the (a) absence and (b) presence of 10 mM CCl_3CO_2H and (c) **2a** in the presence of 10 mM CCl_3CO_2H. The current axes for (a) and (b) are offset by −10 and +20 μA for clarity, respectively. All complexes are 1 mM in CH_3CN/0.1 M (TBA)PF_6. Initial scan direction from the open circuit potential is cathodic in each case. Scan rate: 0.1 V s^{-1}.

In the presence of either H_2O or CCl_3CO_2H, the redox chemistry and, in the case of **2b**, the μ-OH bridge are affected considerably. For **2b**, addition of CCl_3CO_2H or H_2O leads to the formation of **2c**, in which the μ-OH bridge is replaced by a μ-O_2H_3 bridge (Scheme 2; vide infra).

For **2c** $\{Mn^{II}_2(\mu\text{-}O_2H_3)\}$ oxidation is observed at $E_{p,a}$ = 1.03 V (vs SCE, Figure 2a). This process is electrochemically reversible, as can be observed when H_2O or cyclooctene are present with CCl_3CO_2H (vide infra, Figure 7). However, the return waves observed correspond to further chemical reaction of the $\{Mn^{III}_2(\mu\text{-}O_2H_3)\}$ complex formed including formation of **2a**. When 10 equiv of CCl_3CO_2H is added (Figure 2b), the $\{Mn^{II}_2(\mu\text{-}O_2H_3)\}$ to $\{Mn^{III}_2(\mu\text{-}O_2H_3)\}$ two-electron oxidation wave at $E_{p,a}$ = 1.03 V is unaffected; however, only one return wave, a two-electron reduction (Mn^{III}_2 to Mn^{II}_2, at $E_{p,c}$ = 0.67 V), is now observed.

In contrast, for **2b** an electrochemically reversible, one-electron oxidation to $[Mn^{II}Mn^{III}(\mu\text{-}OH)(\mu\text{-}CCl_3CO_2)_2(tmtacn)_2]^{2+}$ is observed at 0.53 V (Figure 3a). Addition of 10 equiv of CCl_3CO_2H to **2b** results in a change of its cyclic voltammetry (Figure 3b) with behavior identical with that of **2c** in the presence of CCl_3CO_2H (Figure 2b). The cyclic voltammetry of **2a** $\{Mn^{III}_2(\mu\text{-}O)\}$ in the absence and presence of CCl_3CO_2H is shown in Figure 4a (i and ii). The effect of addition of CCl_3CO_2H on anodic processes of **2a** (i.e., Mn^{III}_2 to $Mn^{III}Mn^{IV}$ redox process, Table 1) is minimal, even with up to 250 equiv of CCl_3CO_2H (Figure S4) added, confirming that **2a** itself is not protonated under these conditions. However, addition of 1 equiv or more of CCl_3CO_2H to **2a** was found to be sufficient to render the Mn^{III}_2 to $Mn^{II}Mn^{III}$ reduction completely irreversible.

In the presence of CCl_3CO_2H, the reduction at 0.29 V appears to be a 2 e^-/1 H^+ coupled process. The two-electron nature of the reduction wave, apparent from its intensity relative to the Mn^{III}_2 to $Mn^{III}Mn^{IV}$ oxidation waves, may be misleading, however. Instead, the initial reduction step is more probably a H^+/e^- coupled reduction followed by a subsequent one-electron reduction. The irreversibility of the reduction at 0.25 V and the presence of an anodic redox wave at 1.03 V subsequent to reduction of **2a** confirm that a major structural change occurs, i.e., the formation of **2c** (Scheme 2; vide supra).

In the absence of CCl_3CO_2H acid, no redox processes are observed between 0.40 and 1.20 V for **2a**. In the presence of increasing amounts of CCl_3CO_2H, however, the redox wave at $E_{p,c}$ = 0.67 V increases in intensity indicating that the concentration of **2d** is increasing (Figure S4). This indicates that, at higher acid concentrations, the equilibrium between **2a** and **2d** changes in favor of the latter species. In the presence of 10 equiv of CCl_3CO_2H, increasing the H_2O concentration has a similar effect on the cyclic voltammetry of **2a**, confirming that the equilibrium is not dominated by $[H^+]$ or $[CCl_3CO_2H]$ but rather the presence of water, which facilitates opening of the μ-oxido bridge.

Electrochemical Reduction of 1. A key aspect of the catalytic oxidation of alkenes by **1** is the observation of a lag period, at the end of which conversion of **1** to **2a** occurs (vide infra; see Figure 8).[11] In the absence of a proton source the one-electron reduction of **1** is observed at −600 mV (vs SCE).[10c] Although during catalysis the reduction of **1** by H_2O_2 is observed, to facilitate this, **1** must first undergo protonation. In the presence of CCl_3CO_2H the reduction shifts 600 mV anodically and becomes, overall, a four electron reduction process. On the basis of the cyclic voltammetric data, it is apparent that the irreversible reduction of **1** in the presence of CCl_3CO_2H yields, first, **2c** which can undergo subsequent oxidation to form the Mn^{III}_2 complexes **2d** (Figure 5, Scheme 3) and **2a**. Preparative electrochemical reduction of **1** in the presence of CCl_3CO_2H yields **2c** and through subsequent oxidation **2d** (compare signal at 1.09 V in Figure 5a(i) with Figure 2b). The UV−vis spectra of **1** and **2c**,**d** obtained by bulk electrolysis of **1** are shown in Figure 6. As expected for a Mn^{II}_2 complex the absorption spectrum is featureless; however, for **2d** a very intense absorption at

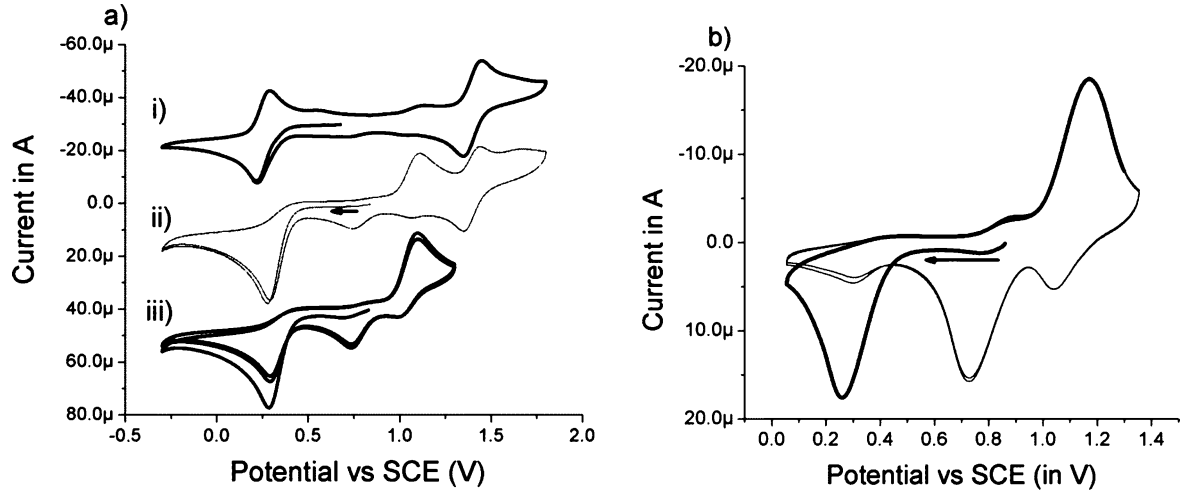

Figure 4. Cyclic voltammetry of **2a** (1 mM) in CH_3CN/0.1 M $(TBA)PF_6$ (a) in the absence (i) and presence (ii) of 10 mM CCl_3CO_2H and (iii) as for (ii) except over a narrower potential window [current axes of the cyclic voltammograms (i) and (ii) offset for clarity] and (b) thin layer cyclic voltammetry of **2a** (1 mM) in the presence of CCl_3CO_2H (10 mM) [initial cycle (thick line); subsequent cycles (thin line)]. When the initial sweep direction is anodic, the process at 1.09 V is not observed for the initial cycle (not shown).

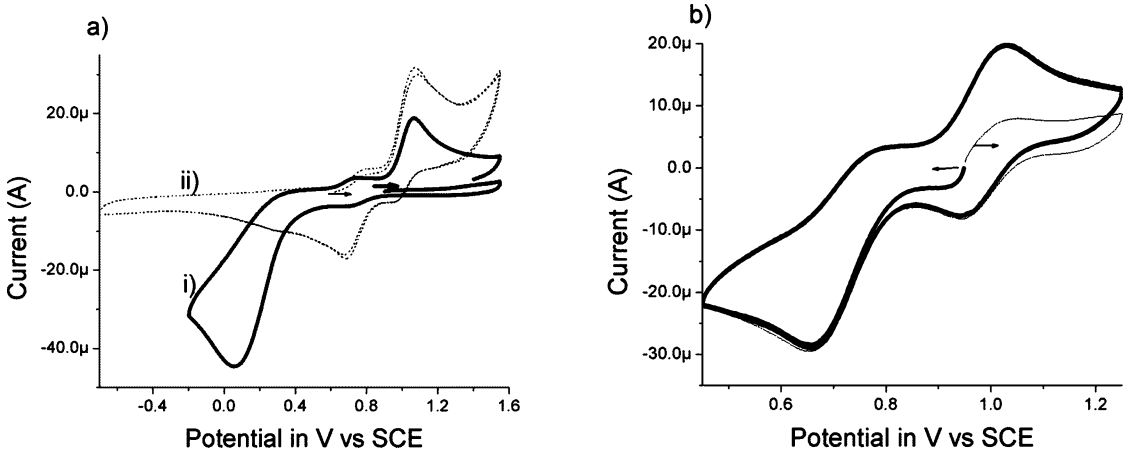

Figure 5. Cyclic voltammetry of **1** in CH_3CN (0.1 M KPF_6) (a) with 10 equiv of CCl_3CO_2H 0.1 V s^{-1} in CH_3CN/0.1 M KPF_6, before (i) and after (ii) bulk reduction at −0.2 V and (b) after reoxidation at 1.10 V [initial scan direction anodic (thin line) and cathodic (thick line)].

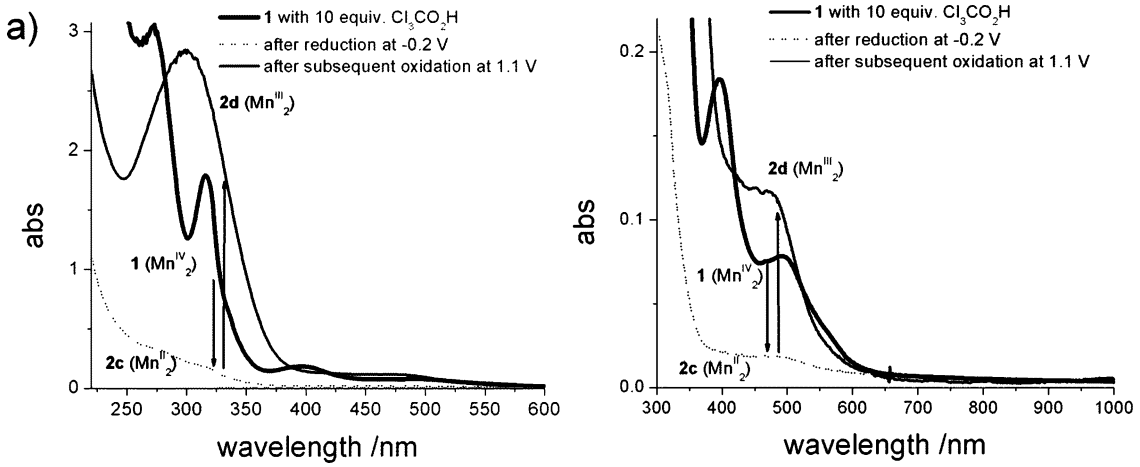

Figure 6. UV−vis spectroscopy of **1** (1 mM) with CCl_3CO_2H (10 mM) in CH_3CN/0.1 M KPF_6: (a) UV−vis spectrum; (b) expansion of visible region before (thick line) and after (dotted line) bulk reduction at −0.2 V and after bulk reoxidation at 1.1 V (thin line).

∼300 nm is observed, together with a weaker absorption at 468 nm. Significantly at 540 nm, the λ_{max} of the absorption of **2a** (Figure 9a; vide infra), **2d** shows only weak absorption (Figure 6). In the presence of acetic acid, in place of CCl_3CO_2H, similar changes are observed; however, oxidation of the Mn^{II}_2 complex formed initially (equivalent to **2c**) yields the μ-oxido-bridged dinuclear complex **3** (Figure S5).

Electrochemistry of 2a−d in the Presence of H_2O_2. In the presence of the substrate cyclooctene, the oxidation ($E_{p,a}$

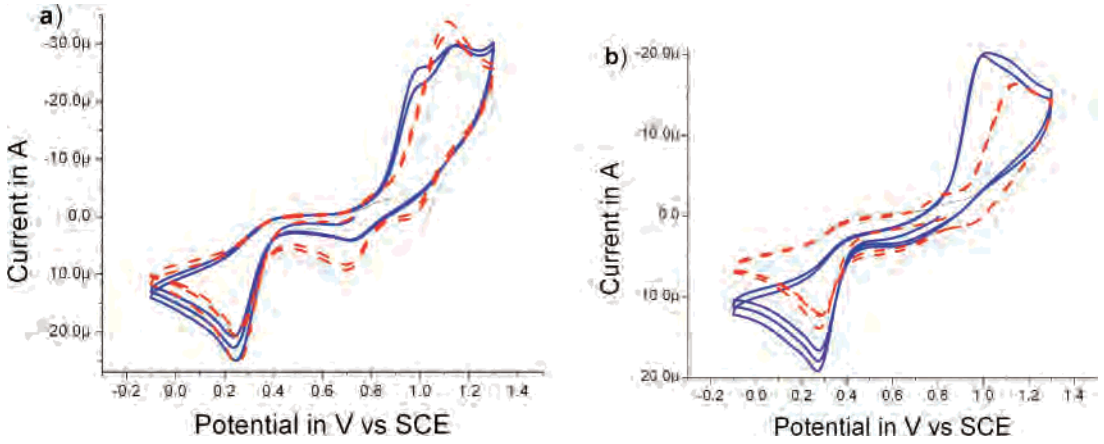

Figure 7. (a) **2a** (1 mM) with 10 equiv of CCl_3CO_2H and 1,2-dichlorobenzene and cyclooctene (1 M) in 0.1 M (TBA)PF_6/CH_3CN: prior to (black/thin line); after ($t \sim 30$ s, blue/thick line) addition of H_2O_2 (50 equiv w.r.t. **2a**) and 20 min after (red/dashed line). (b) As for (a) except without 1,2-dichlorobenzene and cyclooctene.

Scheme 3. Pathways for Conversion of **1** to **2a** by Reduction with H_2O_2 in the Presence of CCl_3CO_2H[26]

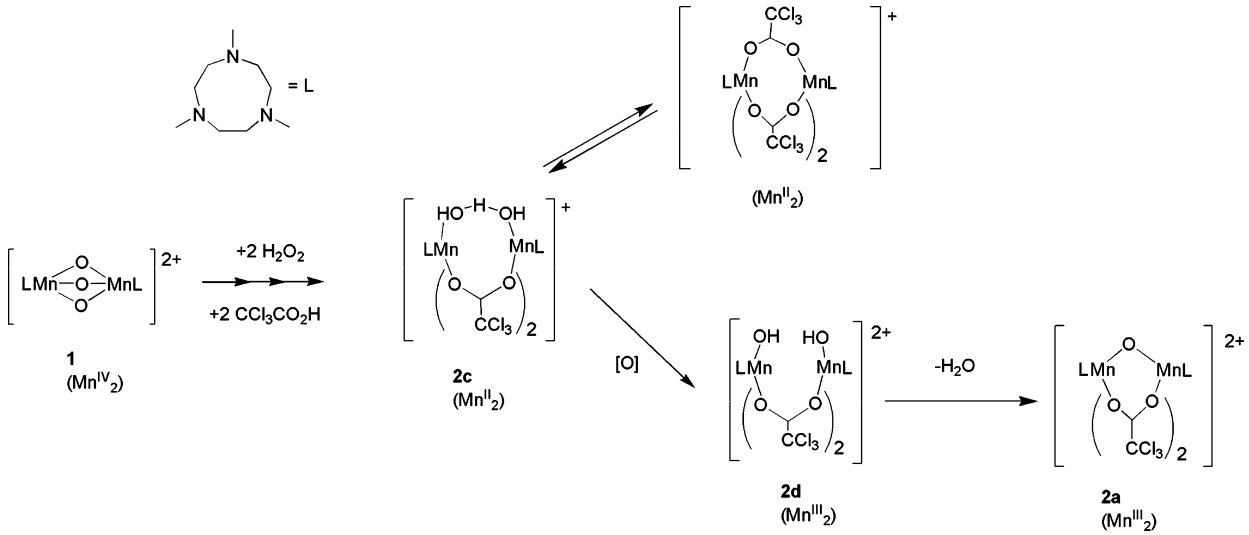

$= 1.09$ V) of **2c** becomes more, albeit not completely, chemically reversible (Figure 7b). Addition of H_2O_2 (both with and without cyclooctene present, Figure 7a,b, respectively) renders the oxidation of **2c** ($E_{p,a} = 1.03$ V) completely irreversible; i.e., the return reduction steps are no longer observed at $E_{p,c} = 0.94$ and 0.67 V. In addition a new irreversible oxidation wave at $E_{p,a} = 0.97$ V is observed, which remains until all H_2O_2 has been consumed. It is reasonable to conclude that this new redox wave is due to ligand exchange of H_2O with H_2O_2 for the complex **2c** (an equilibrium which would benefit from the increased ligand lability expected for a Mn^{II}_2 complex compared with Mn^{III}_2). However, the new oxidation wave is not electrocatalytic in nature; i.e., its intensity is not influenced significantly by the presence of excess H_2O_2 or the presence of an oxidizable substrate. The irreversibility of the oxidation of this new species to a Mn^{III}_2 state results from formation of **2a** rather than **2d**. Indeed it is apparent that complex **2d** reacts with H_2O_2 very rapidly, in stark contrast to **2a** which is largely unaffected by even a 50-fold excess of H_2O_2. The stability of **2a** in the presence of H_2O_2 confirms that the interaction of **2a** with H_2O_2 is a kinetically slow process. The return reduction processes at $E_{p,c} = 0.94$ and 0.67 V (i.e., reduction of **2d**) are observed again after all H_2O_2 is consumed.

UV−Vis, ^{1}H NMR Spectroscopy, and Mass Spectrometry under Catalytic Conditions with 1 and 2a−d. The "standard" reaction discussed in the present paper is the catalytic oxidation of cyclooctene by **1** (0.1 mol %, 1 mM) in the presence of CCl_3CO_2H (10 mM, 1 mol %) at 0 °C in CH_3CN with H_2O_2 (50 w/w % aqueous, 1.3 equiv w.r.t. substrate) added continuously over 6 h, followed by 1 h without addition of H_2O_2.[11,27] The concentration of **1** employed facilitates direct spectroscopic study of the reaction solution. Under these conditions a significant lag period is observed (phase I, Figure 8), after which cis-dihydroxylation and epoxidation begin simultaneously and both processes show similar (up to 4h) time dependence (phase II). Finally, toward the end of the reaction (phase III), the *cis*-diol concentration begins to decrease due to oxidation to the

(27) The addition of water (contained in the 50% H_2O_2) results in phase separation of the reaction mixture, which results in catalyst instability and decomposition to species that can engage in catalase activity. When the H_2O_2 is added in one batch, the selectivity is unaffected; however, substrate conversion is significantly reduced.

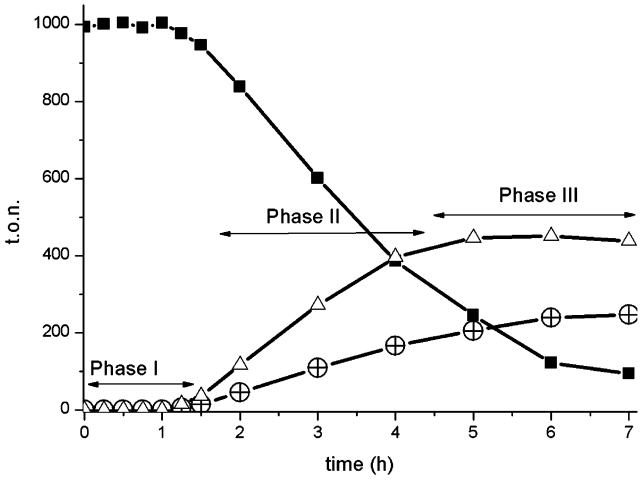

Figure 8. Typical time course for product formation (*cis*-diol, triangles; epoxide, circles) and substrate consumption (cyclooctene, squares) under "standard" conditions (see text for details) in the catalyzed oxidation of cyclooctene with H_2O_2, with **1** (1 mM) and CCl_3CO_2H (10 mM). Key: phase I, lag period; phase II, normal reactivity observed; phase III, subsequent oxidation of *cis*-diol product observed.

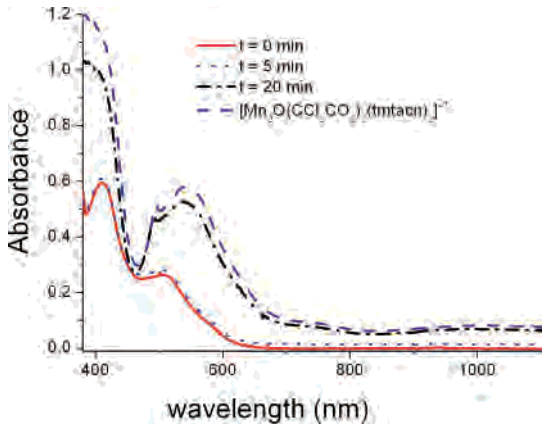

Figure 9. UV−vis spectrum of **2a** (1 mM, blue dashed line) and a mixture of **1** (1 mM)/CCl_3CO_2H (10 mM)/cyclooctene (1 M) after 0 min (red solid line), 5 min (blue dotted line), and 20 min (black dash−dot−dash line) at 20 °C in CH_3CN. [For the full vis−NIR electronic spectra of **2a** and **3** (400−2000 nm), see Figure S9].

corresponding α-hydroxyketone, while the epoxide concentration continues to increase steadily.[11,17n] These distinct phases are observed for all carboxylic acids examined (Figure 1); however, the duration of the lag period and the extent of further oxidation of the *cis*-diol product varies significantly (vide infra, Figure 16).

During the lag period of the reaction (∼30 min at 20 °C and 1 h at 0 °C), no change in either the UV−vis or ESI-MS spectra occurs, and only very weak EPR signals[10c] are observed (vide infra). At the end of the lag period (i.e., the point at which conversion of cyclooctene begins, ∼1 h at 0 °C), both UV−vis spectroscopy and ESI-MS show quantitative conversion of **1** (predominantly to **2a**, Scheme 3, Figure 9). It is also apparent from the intensity of the UV−vis spectrum that the major species (>95%, by comparison with an authentic sample of **2a**) present after the lag period is **2a** (Figure S7).[28] The remainder (<5%), however, is certainly not **1**, as after the lag period **1** is not detectable by either UV−vis or ESI-MS.

^{1}H NMR spectroscopy allows for the direct observation of complexes such as **2a**. However, due to the paramagnetic nature of the Mn^{III}_2 bis(carboxylato) complexes, it is required that nonstandard catalytic conditions are employed to observe spectra of the complexes (Figure S9). Addition of H_2O_2 (20 equiv w.r.t. **1**) to a mixture of **1** (5 mM) and CCl_3CO_2H (50 mM) in acetonitrile results in the quantitative formation of **2a** also, in addition to weaker signals assigned, tentatively, to **2d** $[Mn_2^{III}(OH)_2]^{2+}$. The presence of this latter species, which does not show significant absorbance at 545 nm (the λ_{max} of **2a**), accounts, in part, for the observation of only 85−90% (after 2 h at 20 °C) of the expected signal intensity of **2a** by UV−vis spectroscopy (Figure S7). As with substrate conversion (Figure 8), a lag period of 30 min (60−90 min at 0 °C) is observed for the reduction/ligand exchange of **1** to form **2a** (by UV−vis, Figure 9, and ESI-MS, Figure S8) and the onset of catalytic oxidation (Figure 8 and Scheme 3).

Although the pK_a of **1** is −2,[10c] in acetonitrile containing CCl_3CO_2H (10 mM), a significant amount of the complex is present in the protonated form. The reduction of H**1**$^+$ is, primarily, responsible for the lag period observed prior to the onset of catalytic activity. However as H_2O_2 is incapable of reducing **1** at an appreciable rate even in the presence of a proton source such as HPF_6, it is clear that the formation of the Mn^{II}_2 and Mn^{III}_2 bis(carboxylato)-bridged systems, e.g., **2a**−**d**, results in an autocatalytic reduction of H**1**$^+$ (Figures S7a and S11).[29] Notably the onset of the autocatalytic reaction is delayed by the presence of cyclooctene. Similarly, increased acid concentration above 10 equiv w.r.t. **1** only serves to slow the conversion once initiated. This latter observation can be rationalized by considering that higher acid concentrations favor formation of tris(μ-carboxylato) Mn^{II}_2 species (Figure S3).

Catalytic Oxidation of Cyclooctene with H_2O_2 Catalyzed by 1. The formation of Mn^{III}_2 bis(μ-carboxylato) complexes, such as **2a**, coincides with the onset of catalytic activity of **1**/CCl_3CO_2H. Indeed the formation of the complex in situ by addition of excess H_2O_2 (53 equiv) to **1** (1 mM) and CCl_3CO_2H (10 mM) at 20 °C 20 min prior to addition of cyclooctene and cooling to 0 °C results in a significant reduction in the length of the lag period (Figure 10). This underlines that the formation of **2a** is a prerequisite for catalytic activity (Scheme 3). Overall, the effect of this procedure after 7 h is minor in terms of substrate conversion and *cis*-diol/epoxide ratio (Table S2). However, the incomplete reduction in the lag period, in terms of activity, and the synchronization of the reaction with the standard reaction after 1.5 h indicate that the formation of **2a** is not the sole factor responsible for the lag period.

(28) For all carboxylic acids examined, the formation of the Mn^{III}_2 bis(carboxylato) complexes (i.e. **2a**, **3**−**16**, Figure 1) coincides with initiation of catalytic activity.

(29) The sigmodal shape of the curve showing the formation of **2a** from **1** can be seen in Figures S7 and S11.

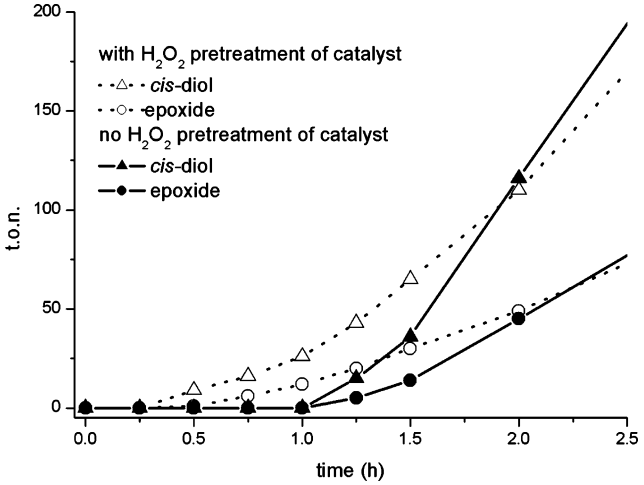

Figure 10. Effect of pretreatment of the catalyst with H_2O_2 prior to addition of substrate on lag period (see text for details).

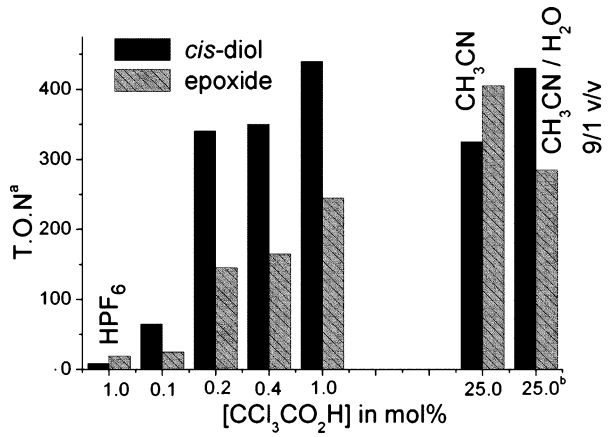

Figure 11. Effect of relative acid concentration on the catalytic oxidation of cyclooctene by **1** (0.1 mol %) at 0 °C: (a) maximum total T.O.N. = 1000; (b) reaction performed in CH_3CN/H_2O (9:1 v/v). See Table S3 for details. Note that although simple proton sources, e.g., HPF_6, together with **1**, are inactive toward cyclooctene oxidation, they are effective in suppressing catalase activity.[31]

Dependence of Catalyst Reactivity and Selectivity on Relative Acid Concentration. The dependence of the activity and selectivity of **1** on the relative concentration of trichloroacetic acid is shown in Figure 11(and Table S3). With less than 2 equiv of CCl_3CO_2H (w.r.t. complex **1**),[11] very low activity is observed. With 2 equiv of CCl_3CO_2H present, a large increase in activity is observed; however, a further increase in acid concentration affects the reaction less, with only a modest increase in activity and increased further oxidation of the *cis*-diol product. Notably, increasing the concentration of acid to 25 mol % results in enhanced selectivity for epoxidation over *cis*-dihydroxylation.

The change in selectivity observed with variation in CCl_3CO_2H concentration is due to solvent water content rather than other effects such as peracid formation (see SI).[6,8,30] Indeed, when CH_3CN/H_2O (9:1 v/v) is used in place of CH_3CN as solvent for the reaction catalyzed by **1** (0.1 mol %) with 25 mol % CCl_3CO_2H, the *cis*-diol/epoxide selectivity increases from 0.79 to 1.5 (Figure 11, and entries VI and VII in Table S3) with a negligible change in overall cyclooctene conversion. The ratio 1.5 is comparable to the ratio 1.8 observed using 1 mol % CCl_3CO_2H, entry IV Table S3. Hence, the difference in selectivity with increasing acid concentration is due to reduction of the effective water content of the reaction mixture.

A central question is the role of the carboxylic acid in controlling the catalysts reactivity and selectivity. That the carboxylic acid acts as a ligand is clear from structural data[11] and the activity and selectivity of **2a** in the absence of additional acid (Table S2, entry III). However, without additional CCl_3CO_2H, the catalyst becomes less active toward the end of the reaction and at ~4.5 h becomes inactive (Figure S10). This loss in activity coincides with a complete decrease in UV−vis absorption of **2a**. The loss in activity is undoubtedly related to the dissociation of the carboxylato ligands from the complex given that in the presence of excess carboxylic acid the activity of the catalytic system is retained,[32] and hence, although excess carboxylic acid is not essential for activity, its presence stabilizes the bis(carboxylato) complexes involved.

Catalytic Oxidation of Cyclooctene with 2a−c. The use of the Mn^{III}_2 complex **2a** and its Mn^{II}_2 analog **2b**, in place of **1**, allows for the near complete elimination of the lag period (Figure 12). However, lower reactivity is observed for **2a** in the first 1.5 h of the reaction compared to the reaction catalyzed by **2b** and during phase II of the reaction (Figure 8).[11]

For both **2b**,**c** a negligible lag period is observed (Figure 12, Table S4), and the activity over the first 1 h with respect to formation of the epoxide product is similar to that observed after 1.5 h. The identical behavior of **2b**,**c** is not, however, surprising, considering that, under reaction conditions (i.e., in the presence of CCl_3CO_2H), **2b** undergoes quantitative conversion to **2c** (vide supra). Under catalytic conditions with either **2b** or **2c**, the *cis*-diol/epoxide ratio is lower over the first 1.5 h of the reaction than observed at later stages of the reaction. The difference in selectivity and the increased reactivity observed for **2c** (and **2b**) compared with **2a** in the early stages (phase I) of the reaction is remarkable considering that within 15 min of the start of the reaction complex **2a** is the predominant species present in solution (80−90% by UV−vis, Figure S7 and Figure S11, and EPR spectroscopy; vide infra). After ca. ~90 min the selectivity of the reaction with **2b** or **2c** is almost identical with that with **1** and **2a**. Furthermore, whether the catalytic oxidation of cyclooctene is performed starting with complex **1**, **2a** [Mn^{III}_2-(μ-O)], **2b** [Mn^{II}_2(μ-OH)], or **2c** [Mn^{II}_2(μ-O_2H_3)], the turnover numbers with respect to both *cis*-diol, epoxide. and the conversion of cyclooctene are very similar (Table S4).

(30) A detailed discussion of this issue is provided in the Supporting Information. See also: (a) Fujitta, M.; Que, L., Jr. *Adv. Synth. Catal.* **2004**, *346*, 190−194. (b) Dubois, G.; Murphy, A.; Stack, T. D. P. *Org. Lett.* **2003**, *5*, 2469−2472. (c) Murphy, A.; Pace, A.; Stack, T. D. P. *Org. Lett.* **2004**, *6*, 3119−3122.

(31) In the presence of HPF_6 (10 equiv), the catalase type activity observed in absence of acid for **1** is substantially inhibited even over a period of 3 h.

(32) At high acid concentrations, tris(μ-carboxylato)-bridged Mn^{II}_2 complexes form in equilibrium with e.g. **2c**, which has an inhibitory effect on the formation of the Mn^{III}_2 species responsible for catalytic activity.

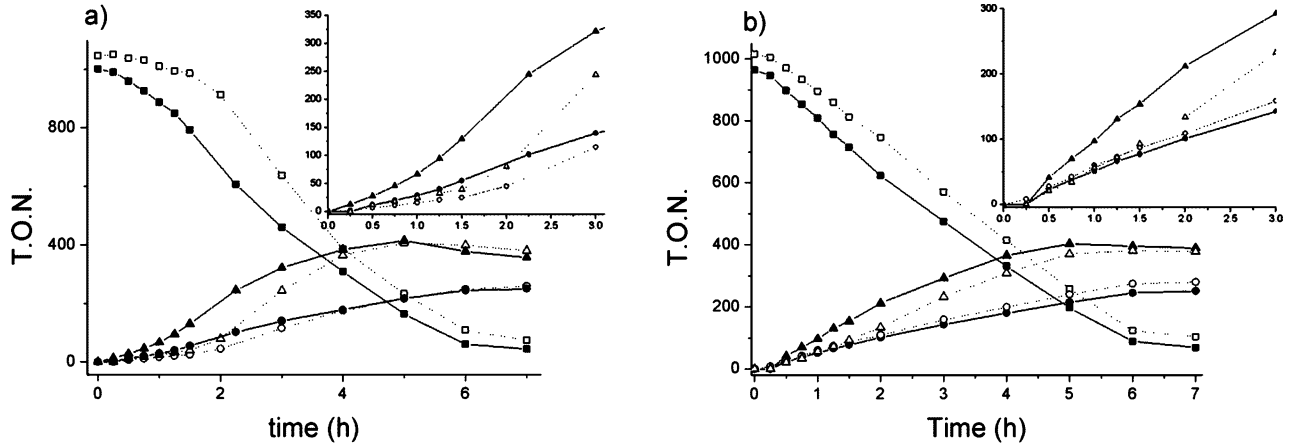

Figure 12. Effect of oxidation state and addition of H_2O prior to start of catalysis on the product distribution in the oxidation of cyclooctene catalyzed by (a) **2a** and (b) **2b**: dotted lines/open symbols, with no H_2O added; solid lines/filled symbols, with added H_2O. Insets: Expansion of first 3 h period (0.1 mol % catalyst, 1 mol % CCl_3CO_2H). Key: cyclooctene/squares; epoxide/circles; *cis*-diol/triangles. See Table S4 for further details.

The origin of the difference in both reactivity and selectivity of the different complexes during phase I of the reaction (Figure 8 and Figure 12) is intriguing and could indicate the presence of a second catalytically active species or catalytic pathway during the early period of the reaction; however, solvent effects should be considered also. During the catalysis, H_2O_2 (50% aqueous solution) is added continuously and, hence, the water content of the reaction mixture increases as the reaction progresses. Indeed addition of H_2O (equal to the amount added over 105 min of catalysis with the added H_2O_2) prior to the start of the reaction catalyzed by either **2a** or **2b** results in a significant difference in the time dependence of product formation observed (Figure 12). Importantly, the *cis*-diol/epoxide ratio for both **2a**,**b** becomes identical with that observed later in the reaction. Furthermore, the reactivity of **2a** is increased to match that observed after 1.5 h. Importantly the level of activity toward epoxidation is affected much less by H_2O addition and the increase in overall activity is due to increased *cis*-diol formation. This latter observation may be related to the ligation strength of *cis*-diols compared to epoxides and, hence, the need to displace *cis*-diol once formed from the catalyst by H_2O (vide infra).

The influence of the water content of the reaction mixture was explored further using H_2O_2/CH_3CN, from which water has been removed (Figure 13).[33] From the time profile of the reaction it is apparent that addition of anhydrous H_2O_2/CH_3CN solution to the reaction mixture with **2a** results in a 1:1 *cis*-diol/epoxide ratio.[34] A control reaction with anhydrous H_2O_2 to which H_2O was added continuously to achieve the same water content as observed normally showed a normal *cis*-diol/epoxide ratio of ca. 2.3.[35] The 1:1 *cis*-diol/epoxide ratios observed during the initial phase of the reaction when using, e.g., **2a** or **2b**, can thus be attributed to the low water content of the reaction mixture during this earlier period rather than to a difference in oxidation state (Mn^{II}_2 vs Mn^{III}_2).

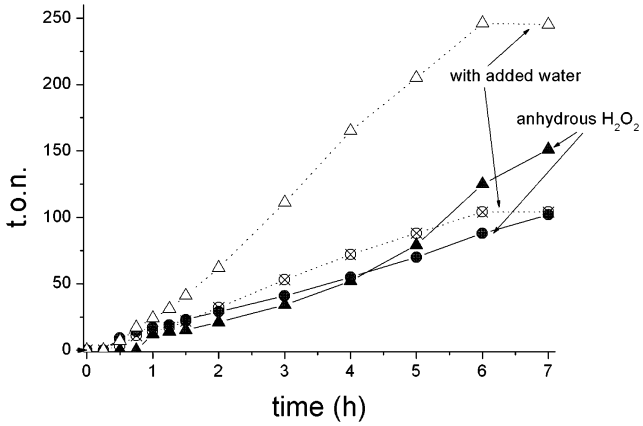

Figure 13. Time course for the formation of *cis*-diol products (triangles) and epoxide (circles) from cyclooctene with anhydrous H_2O_2 (solid lines) and with additional water added with time (dashed lines). H_2O_2 is added at 1/3 the normal amount and rate of addition (see Table S5 for details).

μ-Oxido and μ-Carboxylato Ligand Exchange Rates. Ligand exchange of the μ-oxido bridge of **2a**, **3**, and **7** was followed in time using ESI-MS (see SI for details). For $[Mn^{III}_2(\mu\text{-}^{16}O)(\mu\text{-}CH_3CO_2)_2(tmtacn)_2]^{2+}$ (**3**) relatively slow exchange of the μ-oxido ligand with water-^{18}O was observed (exchange complete within 8 min at rt (room temperature), Figure S12) in $CH_3CN/H_2{}^{18}O$ (9:1) and in the presence of 1 mol % CH_3CO_2H. A rate comparable to that reported recently by Tagore et al. for related dinuclear complexes.[36] For $[Mn^{III}_2(\mu\text{-}^{16}O)(\mu\text{-}2,6\text{-dichloro-benzoate})_2(tmtacn)_2]^{2+}$ (**7**) with 2,6-dichlorobenzoic acid the rate of exchange increased with equilibration complete within 4 min, while for $[Mn^{III}_2(\mu\text{-}^{16}O)(\mu\text{-}CCl_3CO_2)_2(tmtacn)_2]^{2+}$ (**2a**) with CCl_3CO_2H conversion was complete within 1 min, i.e., within the time resolution of the experiment. Notably the rate of ^{18}O

(33) 50% H_2O_2 (w/w H_2O) was diluted in CH_3CN and dried over $MgSO_4$; see ref 30. The use of dry H_2O_2 sources such as UHP was considered; however, practical difficulties, most notably the insolubility of the reagents in CH_3CN, render this approach ineffective in assessing the role of H_2O content.

(34) The increase in *cis*-diol/epoxide ratio observed toward the end of the reaction (ca. 5−7 h) is due to the release of water from H_2O_2 during epoxidation. A reduced rate of H_2O_2 addition (1/3rd normal) was employed to minimize this effect.

(35) The high *cis*-diol/epoxide ratio of 2.3 compared to 1.8 under normal conditions is due to the low level of *cis*-diol overoxidation at low substrate conversion. Under normal conditions a *cis*-diol/epoxide ratio of 2.5 is observed for the same (40%) conversion.

(36) Tagore, R.; Chen, H.; Crabtree, R. H.; Brudvig, G. W. *J. Am. Chem. Soc.* **2006**, *128*, 9457−9465.

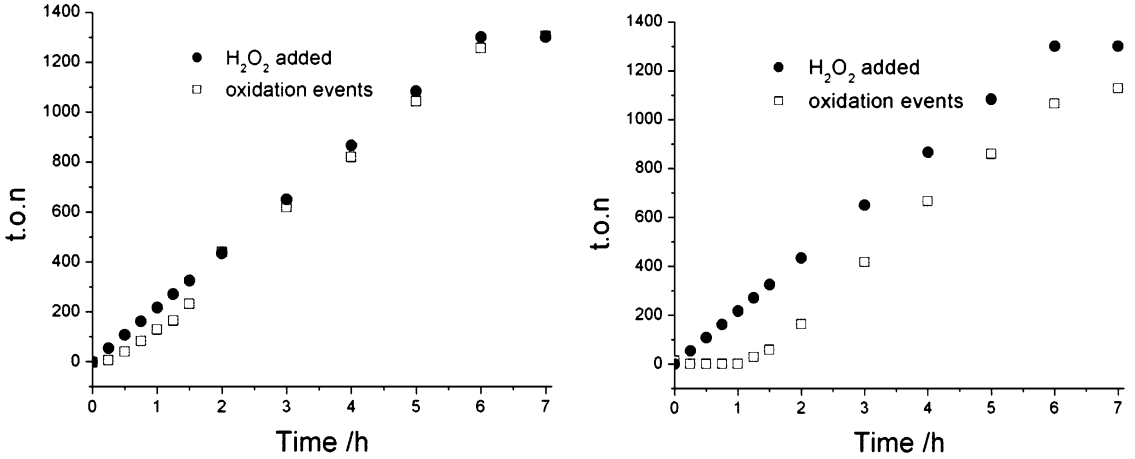

Figure 14. Total number of oxidation events (this is the total T.O.N. for oxidation of cyclooctene + oxidation of the *cis*-diol formed) compared with number of equivalents of H_2O_2 added: (left) **1** (0.1 mol %)/CCl_3CO_2H (1 mol %); (right) **2a** (0.1 mol %)/CCl_3CO_2H (1 mol %) with H_2O (110 μL) added at $t = 0$ (see text for details).

exchange in this latter case is considerably retarded at lower $H_2{}^{18}O$ concentrations.

H_2O_2 Efficiency and the Effect of Lag Period. A key feature of the present system is the atom efficiency with respect to the terminal oxidant (H_2O_2). The efficiency of the reaction, i.e., conversion of substrate and further oxidation of the *cis*-diol with respect to H_2O_2 added, is demonstrated in Figure 14. For the catalytic system **1**/CCl_3CO_2H, the H_2O_2 added during the lag period is consumed only partly during later stages; however, once catalysis commences, the efficiency in terms of oxidant consumption is close to 100%. For **2a**/CCl_3CO_2H, almost all of the oxidant added is used in oxidation of the substrate, albeit with a small amount of H_2O_2 used in the overoxidation of the *cis*-diol, in the final stages of the reaction. The efficiency confirms that a near-complete suppression of catalase type activity occurs. It is of note that the rate of addition H_2O_2 is matched by the consumption of H_2O_2 by the catalyst. This confirms that under the standard conditions employed the turn over frequency is limited by the addition of oxidant[37] and not the intrinsic activity of the catalyst. Indeed under otherwise identical conditions, similar results are obtained over a range of catalyst concentrations (0.38−0.038 mol %) with complete conversion of substrate and similar product ratios.[38] At lower catalyst concentrations (0.0075 mol %) the conversion of substrate is lower (63%, 8400 t.o.n.) and less further oxidation of the *cis*-diol product occurs, leading to a slightly higher *cis*-diol/epoxide ratio.[39]

Solvent Dependence of the Reactivity of 1/CCl_3CO_2H. The influence of solvents other than acetonitrile in the oxidation of cyclooctene was explored, and the results were supported by UV−vis spectroscopy. In ^{t}BuOH/H_2O and THF

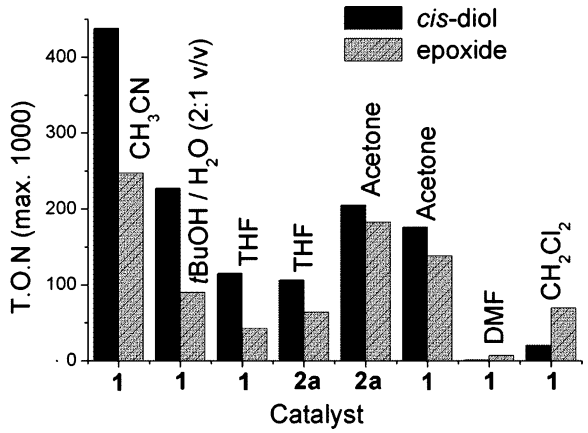

Figure 15. Solvent dependence of the oxidation of cyclooctene after 7 h by **1** or **2a** (0.1 mol %) with CCl_3CO_2H (1 mol %). (See text and Table S6 for further details.)

lower conversion of cyclooctene was observed than that obtained in acetonitrile (Figure 15, Table S6). The higher selectivity toward cis-dihydroxylation in these solvents in comparison to acetonitrile is attributable to the low levels of *cis*-diol overoxidation at low conversion (vide supra). In acetone the formation of acetone/H_2O_2 adducts lowers the effective concentration of H_2O_2 in solution.[40] This has a deleterious effect on the reactivity of **1**/CCl_3CO_2H with H_2O_2 with no activity observed until approximately 4 h,[41] although 46% conversion is observed after 7 h (Table S6). The long lag period at the start of the catalysis is in agreement with the delay in conversion of **1** to **2a** in acetone (by UV−vis spectroscopy). By contrast, when **2a** is used in place of **1**, oxidation activity commences earlier, albeit with a lower *cis*-diol/epoxide ratio than observed in CH_3CN. It should be noted, however, that the low mass balance observed in acetone indicates increased oxidation of the *cis*-diol and hence a lower *cis*-diol/epoxide ratio than is observed for other solvents. Significantly reduced and no activity was observed in dichloromethane and DMF, respectively.

(37) The maximum tof possible under standard conditions is 0.058 s^{-1}.
(38) It should be noted that the dependence of the reaction on the concentration of catalyst, water, and carboxylic acid additive precludes the systematic variation of any single parameter.
(39) This implies that the catalyst turnover frequency is 0.33 s^{-1}. The maximum tof based on the rate of addition of H_2O_2 is 0.77 s^{-1}, suggesting that under these conditions a maximum in catalytic activity is observed; however, this is a lower limit to the tof, as this is calculated over a 7 h period and further oxidation of the *cis*-diol product is not accounted for.
(40) Edwards, J. O.; Sauer, M. C. V. *J. Phys. Chem.* **1971**, *75*, 3004−3011.
(41) The formation of **2a** is observed by UV−vis spectroscopy, ~4 h also.

Table 2. Catalytic Oxidation of Cyclooctene by **2a** (0.1 mol %) at 0 °C in the Presence of Trichloroacetic with $H_2{}^{18}O_2/H_2{}^{16}O$ and $H_2{}^{16}O_2/H_2{}^{18}O$[a]

						T.O.N.	
entry	H_2O	H_2O_2	acid (mol %)	*cis*-diol % $^{16}O^{18}O$	epoxide % ^{18}O	*cis*-diol	epoxide
I	^{16}O	^{18}O	CCl_3CO_2H (1)	103.9	71.2	120	55
II	^{18}O	^{16}O	CCl_3CO_2H (1)	93.0	37.6	105	52
III	^{18}O	^{16}O		79.7	20.8	12	18
IV	^{18}O	^{16}O	CCl_3CO_2H (25)	93.0	33.5	96	50
V[b]	^{18}O	^{16}O	CCl_3CO_2H (1)	94.9	38.2	67	58
VI[c]	^{18}O	^{16}O	CCl_3CO_2H (1)	95	32	427	234

[a] Corrected for H_2O_2/H_2O isotopic composition; see Table S9 for full experimental details). ^{18}O-labeling studies were performed on cyclooctene on 1/20th scale of the standard conditions, with the adjustment that a 2% H_2O_2 solution was used and the peroxide was added batchwise in four portions every 15 min (i.e., at the same rate and amount of H_2O_2 addition under typical reaction conditions). ^{18}Oxygen incorporation was determined by GC-MS (CI) after 60 min reaction time. Values are ±5%. [b] *cis*-2-Heptene as substrate. [c] With 20% H_2O_2(aq) solution.

Overall the solvent dependence of the reactivity of **1**/CCl_3CO_2H correlates well with the stability of complex **2a** under catalytic conditions. That is, catalysis takes place only where **2a** is stable (and can be formed from **1**).[42] Furthermore, the fact that activity is observed in several, quite different solvents (acetone, acetonitrile, ^{t}BuOH/H_2O, THF) indicates that coordination of the organic solvent to the manganese complex is not essential to the catalytic cycle.

Isotopic Labeling Studies. A key probe in "tracking" oxygen atoms in oxidation catalysis is through $^{16}O/^{18}O$ isotope labeling. In this study labeled dihydrogen peroxide ($H_2{}^{18}O_2$) and/or labeled water ($H_2{}^{18}O$) are employed to identify the source of the oxygen atoms incorporated into both *cis*-diol and epoxide products.[43] The lag time observed for, e.g., **1**/CCl_3CO_2H (i.e., the formation of bis(carboxylato)-bridged complexes derived from **1**) was circumvented by using isolated and fully characterized $[Mn^{III}_2(\mu\text{-O})(\mu\text{-carboxylato})_2(\text{tmtacn})_2]^{2+}$ complexes, e.g., **2a**. The results of the labeling studies are given in Table 2.

Under standard reaction conditions (**2a**/1 mol % CCl_3CO_2H) with $H_2{}^{18}O_2$ (2% v/v in $H_2{}^{16}O$), single ^{18}O incorporation in the *cis*-diol product is observed, while ^{18}O incorporation in the epoxide product is 71%. For the complementary experiment with $H_2{}^{16}O_2$ (2% v/v in $H_2{}^{18}O$), again single ^{18}O incorporation in the *cis*-diol product and 38% ^{18}O incorporation in the epoxide product is found. Very similar results were obtained in the cis-dihydroxylation/epoxidation of *cis*-2-heptene (Table 2, entry V).[44]

Interestingly, at 25 mol % CCl_3CO_2H, no significant difference in ^{18}O incorporation in either the *cis*-diol or epoxide product is observed compared with the reaction with 1 mol % CCl_3CO_2H (entry IV); however, in the absence of trichloroacetic acid (using **2a** as catalyst), reduced ^{18}O incorporation from $H_2{}^{18}O$ into the *cis*-diol (single incorporation, 80%) and the epoxide (21%) is observed, as well as greatly reduced conversion (vide supra and Table S9).

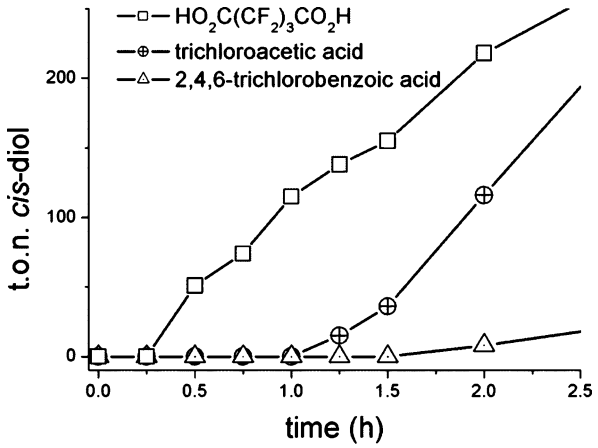

Figure 16. Time dependence of *cis*-diol formation for $HO_2C(CF_2)_3CO_2H$, CCl_3CO_2H, and 2,4,6-trichlorobenzoic acid promoted catalytic oxidation of cyclooctene by **1** (standard conditions).

The use of D_2O_2/D_2O in place of H_2O_2/H_2O resulted in no significant changes to either the time dependence of product formation or the overall conversion (Table S7), indicating that proton (or hydrogen atom) transfer does not play a role in the rate-determining step of the reaction.

Tuning of the Activity and Selectivity by Variation in Carboxylate Ligands. Although in general both aliphatic and aromatic carboxylic acids promote the oxidation of cyclooctene to both *cis*-diol and epoxide with H_2O_2 by **1**, the duration of the lag period (Figure 16), the *cis*-diol/epoxide ratio, and the conversion are dependent on the specific carboxylic acid employed (Table S8). For example, for hexafluoroglutaric acid a lag time of only 15−30 min is observed at 0 °C, while for 2,4,6,-trichlorobenzoic acid a lag period of 2−3 h was observed (Figure 16 and Table S8). Hence, in comparing the activity of carboxylic acids, it is important to take the lag period into consideration, as an apparent low activity can be due to slow formation of the bis(carboxylato)-bridged dinuclear complex rather than an intrinsically low reactivity.

Since the primary species present in solution during catalysis are Mn^{III}_2 species such as **2a**,**d**, ditopic carboxylato ligands (i.e., glutaric and hexafluoroglutaric acid) were examined for activity and the duration of the lag period also (Table S8). Both the activity and selectivity of these two

(42) It should be noted that the absence of activity or reduced activity observed in different solvents can, potentially, be due to competitive solvent oxidation which leads to a reduced efficiency in terms of cyclooctene conversion. However, catalytic activity toward alkene oxidation was observed only when **2a** was present in solution.

(43) A difficulty arises, however, in the availability of $H_2{}^{18}O_2$ as a 2% v/v solution in contrast to the 50% w/w H_2O_2 solution employed in typical catalysis experiments. However, since the presence of water in the reaction medium allows for "normal" catalysis to take place, the relatively large amount present in the labeling studies is not considered problematic. In addition, the *cis*-diol/epoxide ratios obtained at several H_2O_2/H_2O ratios (50, 30, 20, and 2%) indicate no significant difference in the chemistry observed under labeling conditions compared with standard reaction conditions.

(44) Overall, the spectral features of the reaction solution are unaffected by variation in substrate.

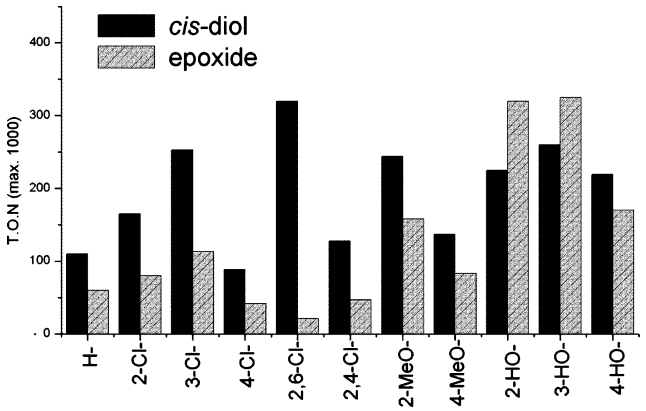

Figure 17. Cis-dihydroxylation and epoxidation of cyclooctene by **1** (0.1 mol %) in the presence of selected methoxy-, chloro-, and hydroxy-substituted benzoic acids (1 mol %). See also Tables S2 and S8.

carboxylic acids are comparable with their mono(carboxylic acid) counterparts (acetic and trifluoroacetic acid, respectively). For hexafluoroglutaric acid a shorter lag period is observed compared with trifluoroacetic acid. For glutaric acid, however, the increased activity observed compared with acetic acid is somewhat surprising, when it is considered that glutaric acid exhibits a much longer lag period. That the ligands are ditopic is apparent from mass spectral analysis, and hence, an increased effective local concentration of carboxylic acid may be responsible for the increased activity observed. It is worth noting, however, that for the glutarato-bridged complex **4** formation of the "oxido-bridge-opened" Mn^{III}_2 complex (analogous **2d**) is more pronounced than observed for the acetate-bridged complex **3** (by electrochemistry and ^{1}H NMR spectroscopy), and hence while in the Mn^{III}_2 state this will facilitate coordination of H_2O_2, in the Mn^{II}_2 state it will also encourage formation of tris(μ-carboxylato)-bridged complexes which inhibits conversion of **1** to **4** and hence extends the lag period observed.

For benzoic acid and its F-, Cl-, HO-, MeO-, and Me-substituted analogs, activity toward both cis-dihydroxylation and epoxidation are observed and selected data are presented in Figure 17 (for a more comprehensive data set, see Table S8). Several inferences regarding the relative importance of steric and electronic effects toward reactivity and selectivity can be drawn. With the exception of 2,4,6-trimethyl- and 4-chlorobenzoic acid, for all substituted benzoic acids examined, an increase in activity compared with benzoic acid is observed. Comparison of *ortho*-, *meta*-, and *para*-mono-substituted benzoic acids shows only minor differences in selectivity; however, overall *para*-substitution results in a significant decrease in activity. For the substituted benzoate based complexes, there appears to be no clear correlation between electronic parameters and either activity or selectivity. However, it should be noted that, in contrast to the aliphatic acids (e.g., acetic and trichloroacetic acid), the effect of substitution on the redox properties of the complexes is relatively minor (Table S1) and the activity observed is affected significantly by the length of the lag period.

Importantly, the selectivity of the reaction shows only moderate sensitivity to the position of the HO$-$ group in the hydroxybenzoic acid series (i.e. *meta*-OH $\sim$ *ortho*-OH) indicating that, in the case of 2-hydroxybenzoic acid, coordination of the proximal $-$OH group to the manganese centers does not occur under catalytic conditions.[45] By contrast, steric demands appear to be more important with regard to selectivity, with 2,6-disubstituted benzoic acids providing consistently higher *cis*-diol/epoxide ratios without loss in activity, compared with their *ortho*-mono-substituted analogs. For instance, with 2,6-difluorobenzoic acid, the activity is comparable to that with 2,6-dichlorobenzoic acid but the selectivity observed was comparable to that with benzoic acid. Furthermore, for the 2,4,6-trimethylbenzoic acid promoted reaction, although very low reactivity is observed, the *cis*-diol/epoxide selectivity is high ($\sim$5, Table S8). This suggests that while the activity is driven by both electronic and steric effects, the selectivity is dominated by steric factors.

As with **2a** (vide supra), for other μ-carboxylato-bridged complexes (i.e., 2,6-dichloro- (**7**), 2,4-dichloro- (**6**), 4-hydroxy- (**9**), and 2-hydroxybenzoato (**8**)), ^{18}O incorporation from $H_2{}^{18}O$ into the *cis*-diol product is relatively insensitive to the nature of the acid (82$-$94%, single oxygen incorporation from the H_2O_2); however, for the epoxide product the extent of ^{18}O incorporation from $H_2{}^{18}O$ ranges from 3 to 38% depending on the complex/carboxylic acid employed (Table 2 and Table 3).

EPR Spectroscopy of 1/CCl_3CO_2H and 2a$-$c under Reaction Conditions. EPR spectroscopy presents a powerful tool in the study of manganese-based catalytic systems. Although, from UV$-$vis spectroscopy and mass spectrometry it is clear that the major species present in solution are EPR-silent Mn^{III}_2 dinuclear complexes, such as **2a** ([Mn^{III}_2(μ-O)(μ-CCl_3CO_2)$_2$(tmtacn)$_2$]$^{2+}$), the availability of EPR-active (Mn^{II}_2) complexes such as **2b**,**c** allows for assessment of their involvement during catalysis.[46]

The EPR spectra of both **2b**,**c**[47] in acetonitrile (1 mM at 77 K, Figure 18a) are characterized by very broad features at $g \sim 2$, which do not show discernible hyperfine splitting (except in the presence of cyclooctene; vide infra). The spectra of **2b**,**c** bear a remarkable similarity to that of the dinuclear manganese(II) catalase enzyme from *T. Thermophillus* reported by Dismukes and co-workers with peak to peak separations of 530 G and a hyperfine splitting of 45 G.[48] As observed by cyclic voltammetry (vide supra), addition of 10 equiv of CCl_3CO_2H to **2b** results in the appearance of a spectrum identical with that of **2c**. The spectrum of **2c** itself in CH_3CN is unaffected by addition of CCl_3CO_2H. However, addition of cyclooctene to a solution of **2c** in CH_3CN leads to the formation of a mixture of **2b**,**c**.

For **2c** broad signals are observed in acetonitrile; however,

(45) The mononuclear Mn^{III} complex **8** converts to a bis(carboxylate)-bridged complex under catalytic conditions.[11]

(46) A detailed analysis of the magnetic properties including temperature dependence and fitting is beyond the scope of the present discussion and will be reported elsewhere.

(47) The spectrum is very similar to that of a structurally related complex based on the bpea (*N*,*N*′-bis(2-pyridylmethyl)ethylamine) ligand. See: Romero, I.; Dubois, L.; Collomb, M.-N.; Deronzier, A.; Latour, J.-M.; Pécaut, J. *Inorg. Chem.* **2002**, *41*, 1795$-$1806.

(48) Pessiki, P. J.; Khangulov, S. V., Ho, D. M.; G. C. Dismukes, *J. Am. Chem. Soc.* **1994**, *116*, 891$-$897.

Table 3. $^{16/18}O$ Isotopic Distribution in the Oxidation Products of Cyclooctene by $[Mn^{III}_2(\mu\text{-O})(\mu\text{-carboxylato})_2(tmtacn)_2]^{2+}$ Complexes (0.1 mol %) at 0 °C in the Presence of the Corresponding Carboxylic Acid with $H_2{}^{16}O_2/H_2{}^{18}O$ (Corrected for H_2O_2/H_2O Isotopic Composition)[a]

							T.O.N.	
entry	H_2O	H_2O_2	catal (0.1 mol %)	acid (mol %)	*cis*-diol % $^{16}O^{18}O$	epoxide % ^{18}O	*cis*-diol	epoxide
I	^{18}O	^{16}O	**6**	2,4-dichlorobenzoic acid (1)	89.8	13.4	60	24
II	^{18}O	^{16}O	**6**	2,4-dichlorobenzoic acid (25)	93.9	11.0	109	40
III	^{18}O	^{16}O	**7**	2,6-dichlorobenzoic acid (3)	92.8	18.6	115	12
IV	^{18}O	^{16}O	**9**	4-hydroxybenzoic acid (1)	86.4	11.6	20	37
V	^{18}O	^{16}O	**8**	2-hydroxybenzoic acid (1)	81.6	3.1	23	50

[a] ^{18}O-labeling studies were performed on cyclooctene on 1/20th scale of standard conditions, with the adjustment that a 2% H_2O_2 solution was added batchwise in four portions every 15 min (i.e., at the same rate and amount of H_2O_2 addition under typical reaction conditions). See Table S9 for full experimental details.

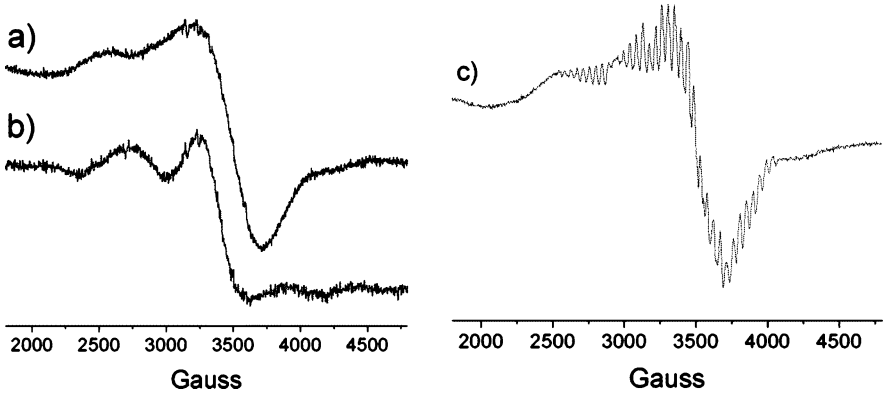

Figure 18. EPR spectra (X-band at 77 K) of (a) **2c** in CH_3CN (1 mM, 77 K), (b) **2b** (1 mM) in CH_3CN/1 M cyclooctene, and (c) **2b** (1 mM) in CH_3CN/1 M cyclooctene with 10 equiv of CCl_3CO_2H acid. Recording conditions: microwave power, 63 mW; modulation amplitude, 0.1 mT; modulation frequency, 50 kHz; time constant, 81.92 ms; *T*, 77 K; 9.47 GHz.

a decrease in solvent polarity by addition of cyclooctene, although not affecting the overall shape and intensity of the spectrum, leads the appearance of a distinct hyperfine-coupling pattern ($a = 43$ G, Figure S13).[49] The observation of a solvent polarity dependence on the resolution of the hyperfine structure for **2c** is in agreement with the assignment of a μ-O_2H_3 bridging unit being present (Figure 1). Furthermore, for **2b**[50] in the presence of both cyclooctene *and* 10 equiv of CCl_3CO_2H, an identical spectrum is observed, again showing fine structure with hyperfine splitting ($a = 43$ G, Figure 18c).

The oxidation of cyclooctene by H_2O_2 catalyzed by **1** (1 mM) in the presence of CCl_3CO_2H (10 mM) at 20 °C was followed by EPR spectroscopy under standard catalytic concentrations. After 15 min, a multiline signal is observed (attributed to **2c** present at low concentrations, vide supra), present at low concentrations (Figure S14).[51] This weak signal decreases in intensity over the first 1 h of the reaction with the appearance of a very weak 6 line signal ($a = 90$ G).[52] Interestingly, a weak signal, assigned to **2c**, is observed in the EPR spectrum of **2a** (1 mM), in cyclooctene/CCl_3CO_2H (10 mM)/CH_3CN, prior to addition of H_2O_2. Addition of H_2O_2 results in the disappearance of this signal. After 45 min the appearance of a very weak 6 line signal is observed (a Mn^{II}−carboxylato complex dissociated from tmtacn, $a = 90$ G).[52]

In summary, by EPR spectroscopy the conversion of **2b** to **2c** in the presence of CCl_3CO_2H and the subsequent conversion of **2c** to an EPR-silent complex (i.e., **2a**) upon addition of H_2O_2 is observed (Figure S14c). Overall, although several species are observed by EPR spectroscopy, namely **2c** (Figure S16) and free mononuclear Mn^{II}−tris(carboxylato) complexes,[52] the EPR signal is weak during catalysis, in agreement with electrochemical, ESI-MS, and UV−vis spectroscopic studies in which the major species observed is the EPR-silent Mn^{III}_2 complex **2a**.[53]

(49) The nature of the bridging μ-H_3O_2 unit is currently under further investigation. For similar examples of this structural motif, see the following: (a) Stibrany, R. T.; Gorun, S. M. *Angew. Chem., Int. Ed. Engl.* **1990**, *29*, 1156−1158. (b) Boudalis, A. K.; Lalioti, N.; Spyroulias, G. A.; Raptopoulou, C. P.; Terzis, A.; Bousseksou, A.; Tangoulis, V.; Tuchagues, J.-P.; Perlepes, S. P. *Inorg. Chem.*, **2002**, *41*, 6474−6487. (c) Jaime, E.; Weston, J. *Euro. J. Inorg. Chem.* **2006**, 793−801. (d) Meyer, F.; Rutsch, P. *Chem. Commun.* **1998**, 1037−1038. (e) De Munno, G.; Viterbo, D.; Caneschi, A.; Lloret, F.; Julve, M. *Inorg. Chem.*, **1984**, *33*, 1585−1586. (f) Dong, Y.; Fujii, H.; Hendrich, M. P.; Leising, R. A.; Pan, G.; Randall, C. R.; Wilkinson, E. C.; Zang, Y.; Que, L., Jr.; Fox, B. J.; Kauffmann, K.; Munck, E. *J. Am. Chem. Soc.* **1995**, *117*, 2778−2792. (g) Ardon, M.; Bino, A.; Michelsen, K.; Pedersen, E.; Thompson, R. C. *Inorg. Chem.* **1997**, *36*, 4147−4150.

(50) For **2b** a decrease in solvent polarity by addition of cyclooctene alone does not affect the EPR spectrum (Figure 18).

(51) On the basis of intensity compared with **2c** (1 mM) under identical conditions.

(52) At higher concentrations (5 mM **1**/50 mM CCl_3CO_2H) in butyronitrile/acetonitrile, although not affecting the outcome of the catalysis significantly (Figure S15), the appearance of the multiline signal assigned to **2c** is more pronounced; however, again a steady-state concentration is reached after 30 min and after 2 h the multiline signal disappears again, replaced by a six line signal typical of mononuclear Mn^{II}. The increased intensity of the Mn^{II} mononuclear signal is due in part to the overall increase in concentration but also to the increased acid concentration. The mononuclear species is assigned, tentatively, as $[Mn^{II}(CCl_3CO_2)_3]^-$ on the basis of comparison with $Mn^{II}(ClO_4)_2$/CCl_3CO_2H (1:10) in CH_3CN and the observation of the ion in negative mode ESI-MS. $Mn^{II}(ClO_4)_2$/CCl_3CO_2H (1:10) is inactive under the reaction conditions employed in the present study; see Table S11, entry VI.

Scheme 4. Summary of Process Which Occur during Phases I−III[a]

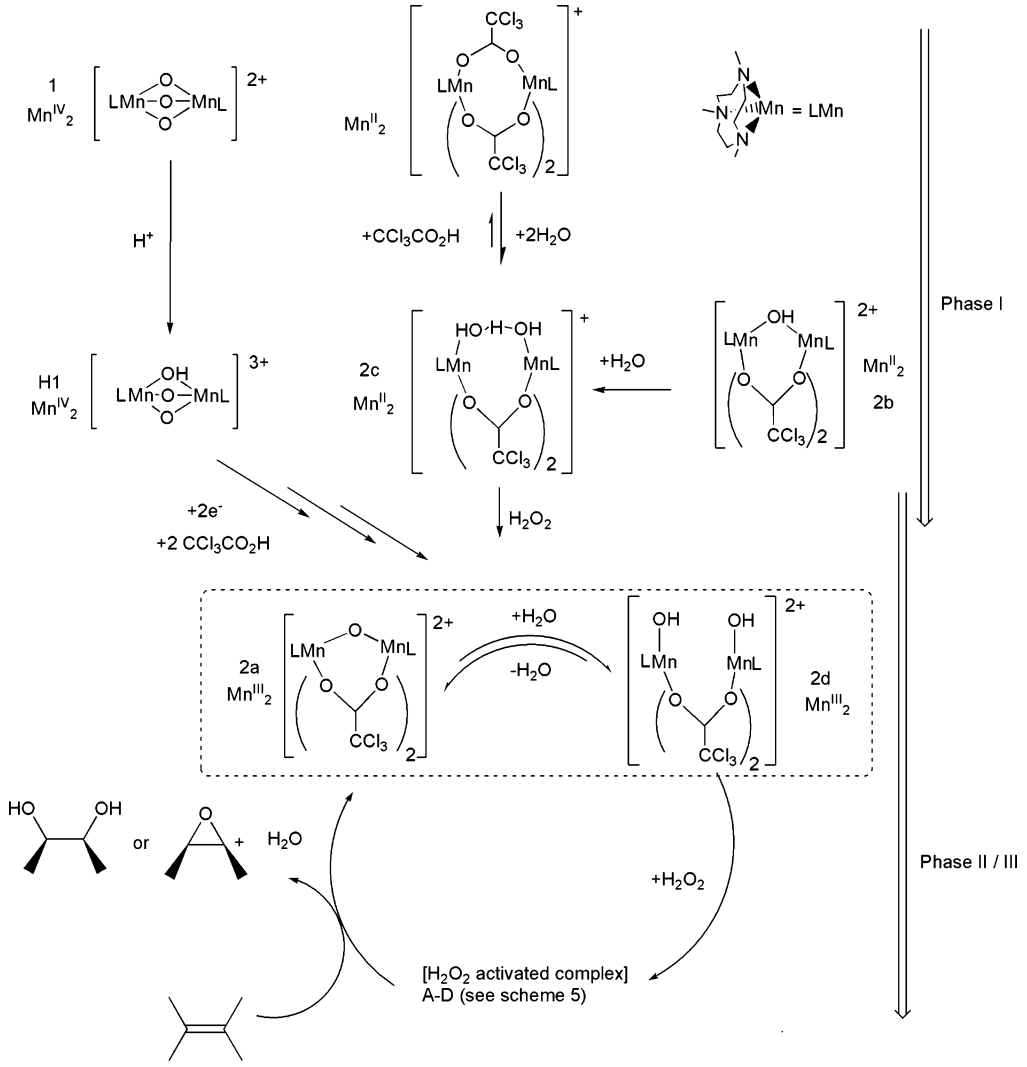

[a] See Figure 8.

Overall it is apparent that although the formation of Mn^{II}_2 and Mn^{III}_2 bis(μ-carboxylato) species occurs at least within 30 min of initiation of addition of H_2O_2 to the reaction mixture, the initiation of catalytic activity is observed only when the Mn^{III}_2 bis(μ-carboxylato) complexes, e.g., **2a**, **7**, etc., form.

Overview of Complex Formation and of Oxidation Processes. A summary of the complexes involved in the catalytic system is provided in Scheme 4. In the carboxylic acid promoted catalytic oxidation of alkenes by **1**, the first step is reduction of $H\mathbf{1}^+$ by H_2O_2 and ligand exchange to form **2a**. Hence, the use of dinuclear manganese bis(μ-carboxylato) complexes, either prepared or generated in situ prior to initiation of catalysis, results in the elimination of the lag period observed with **1**.

Under reaction conditions, prior to addition of H_2O_2, the Mn^{II}_2 complex **2b** is converted quantitatively to **2c**, and upon addition of H_2O_2, almost complete conversion to **2a** is observed within the first 5 min of the reaction. Although Mn^{II}_2 complexes, i.e., $[Mn^{II}_2(\mu\text{-}O_2H_3)(\mu\text{-}RCO_2)_2(tmtacn)_2]^{2+}$ (cf. **1**/dichlorobenzoic acid), may be present during the lag period for some of the carboxylic acids examined, the onset of catalytic activity does not coincide with their formation. Furthermore, the observation that **2c** can interact with H_2O_2 to form a metastable complex (as observed by electrochemistry) supports the conclusion that Mn^{II}_2 complexes are not involved in the catalytic cycle directly.

Regardless of the various processes that occur prior to the onset of catalytic activity, it is certain that catalysis is observed only where either **2a** or **2d** is present in solution. In the presence of H_2O_2, **2d** is not observed until all H_2O_2 has been consumed (see Figure 7), whereas the concentration of **2a** is relatively unaffected by the addition of H_2O_2. Hence, it is reasonable to propose that the species which interacts with H_2O_2 is the dinuclear Mn^{III}_2 complex, **2d**. The preponderance of **2a** in solution (>85−95% depending on conditions) compared with **2d** suggests that **2a** is directly involved in the catalytic cycle and that the opening of the μ-oxido bridge of **2a** is limiting reactivity. That is, **2a** acts as a catalyst resting point, which is in equilibrium with **2d** (Scheme 4).

(53) Similar results were obtained for the reaction catalyzed by **1** with 2,6-dichlorobenzoic acid. See the SI for details.

Coordination of H_2O_2 to **2d** is followed by reaction of the H_2O_2 activated species with the substrate to re-form **2a**.

The primary role of H_2O in determining activity appears to be the formation of **2d**. The equilibrium between **2d**, which interacts with H_2O_2, and **2a** is affected strongly by both the amount of H_2O present and the carboxylic acid concentration. That this is the case is further supported by comparison of glutaric and acetic acid promoted reactions. In the case of the glutaric acid based complex **4**, formation of the $Mn^{III}_2(OH)_2$ species (analogous to **2d**) occurs much more readily than for the corresponding acetate-bridged complex **3**, and the glutarato-bridged complexes show much higher reactivity than the corresponding acetato complexes, despite being "electronically" equivalent. Furthermore from ESI-MS ^{18}O labeling studies (vide supra), it is clear that the rate of exchange of the μ-oxido bridge of the Mn^{III}_2 bis-(carboxylato) complexes is dependent on the nature of the μ-carboxylato ligands with the rate increasing with increasing electron-withdrawing character of the ligand.

Hence, both **2a**,**d** can be implicated directly in the catalytic cycle, and the rate-determining step in the reaction is the formation of **2d** from **2a**. Furthermore, once formed, **2d** interacts with H_2O_2 followed by oxidation of the substrate to re-form **2a**.

Mechanistic Considerations. Although two complexes in the catalytic cycle, i.e., **2a**/**2d**, have been identified experimentally, a key question now arises; are two catalytically active species involved *(*one for cis-dihydroxylation and one for epoxidation), or if a common H_2O_2 activated intermediate is responsible for both oxidation processes, what is the nuclearity and nature of such a species?

Several aspects of the current catalytic system indicate that a common intermediate is involved or at least that there is a common immediate precursor to the species responsible for *cis*-diol and epoxide formation, respectively. First, the conversion of cyclooctene to *cis*-diol and epoxide commences simultaneously and the processes which change the duration of the lag period (e.g., catalyst preactivation, initial oxidation state of the catalyst, H_2O content of the reaction mixture, etc.) all effect the lag time for both cis-dihydroxylation and epoxidation in the same manner. Second, both cis-dihydroxylation and epoxidation show similar time dependence over the course of the reaction. Significantly lower *cis*-diol/epoxide ratios are observed during the initial stages of the reaction when either the well-defined complexes **2a**−**c** are used as catalysts or high acid concentrations are employed. However, this decrease is due to the low water content of the reaction mixture during the early stages and the "dehydrating" effect of high acid concentrations since addition of H_2O restores normal catalytic behavior. Hence, any reaction mechanism should take into consideration a common catalyst being, most probably, responsible for both cis-dihydroxylation and epoxidation.

The majority of mechanisms, proposed previously for the tmtacn family of manganese catalysts, have favored the formation of mono- and dinuclear high-valent oxidizing species,[54] albeit with relatively scant empirical evidence to support such proposals. In the most detailed study available

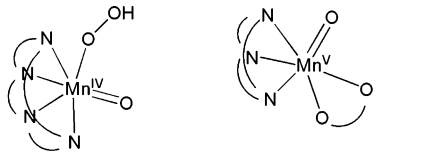

inorganic peracid proposed by Busch and coworkers

Mn(V)=O proposed by Lindsay-Smith and coworkers

Figure 19. Proposed structures for H_2O_2-activated manganese complexes.[55,58]

to date, based on ESI-MS, mononuclear high-valent Mn^{IV}=O and Mn^{V}=O species[55] were proposed by Lindsay-Smith and co-workers during the oxidation of phenols and the epoxidation of cinnamic acid[56] derivatives by Mn^{II}−tmtacn (in the presence of oxalic acid and other additives) (Figure 19).[57] Recently, in a related tetraazabicyclohexadecane-based system Busch and co-workers[58] have suggested a mononuclear Mn^{IV} peroxy complex (LMn^{IV}(=O)OOH, where L = 4,11-dimethyl-1,4,8,11-tetraazabicyclo[6.6.2]hexadecane) as being the activated oxidant in the epoxidation of olefins, a so-named inorganic peracid.[59] On the basis of these studies, it is tempting to postulate that a mononuclear active species is operating in the present systems also.

However, despite extensive spectroscopic and electrochemical characterization of the present system, such mononuclear species have never been observed. While that does not exclude their involvement completely, this fact requires that we consider also a mechanism which recognizes that throughout the reaction >95% of the manganese is present in solution as dinuclear Mn^{III}_2 complexes (e.g., **2a**,**d**). Furthermore, the number of turnovers that the catalyst can undergo during catalysis (>2500)[11] and the absence of spectroscopic evidence for any H_2O_2-activated complexes during catalysis indicate that the rate-determining step in the catalytic cycle involves formation of **2d** from **2a**. Subsequent coordination of H_2O_2 to **2d** takes place followed by rapid reaction of the activated complex (Scheme 4). In addition the re-formation of **2a**, after oxidation of the substrate, is fast and virtually complete. Overall the inability of peroxide either to reduce or oxidize the Mn^{III}_2 dinuclear complex **2a**

(54) For recent reviews, see the following: (a) Sibbons, K. F.; Shastri, K.; Watkinson, M. *Dalton Trans.* **2006**, 645−661. (b) Hage, R.; Lienke, A. *J. Mol. Catal. A* **2006**, *251*, 150−158.

(55) In this work, no such species have been identified either by UV−vis, ESI-MS, or EPR spectroscopies. In particular, no signals were observed at 1600 G ($g = 4$) typical of either a mono- or dinuclear Mn^{IV} species.

(56) From Hammett parameters on a series of substituted cinnamic acid derivatives, it was concluded that the active species is electrophilic in nature, and ^{18}O-labeling study showed incorporation of oxygen in the epoxide from H_2O (ca. 10%) in addition to incorporation from H_2O_2 (ca. 90%) using oxalic acid as additive: Gilbert, B. C.; Lindsay Smith, J. R.; Mairata i Payeras, A.; Oakes, J.; Pons i Prats, R. *J. Mol. Catal., A: Chem.* **2004**, *219*, 265−272.

(57) Gilbert, B. C.; Smith, J. R. L.; Mairata i Payeras, A.; Oakes, J. *Org. Biomol. Chem.* **2004**, *2*, 1176−1180.

(58) (a) Yin, G.; Buchalova, M.; Danby, A. M.; Perkins, C. M.; Kitko, D.; Carter, J. D.; Scheper, W. M.; Busch, D. H. *Inorg. Chem.* **2006**, *45*, 3467−3474. (b) Yin, G.; Buchalova, M.; Danby, A. M.; Perkins, C. M.; Kitko, D.; Carter, J. D.; Scheper, W. M.; Busch, D. H. *J. Am. Chem. Soc.* **2005**, *127*, 17170−17171.

(59) Deubel, D. V.; Frenking, G.; Gisdakis, P.; Hermann, W. A.; Rosch, N.; Sundermeyer, J. *Acc. Chem. Res.* **2004**, *37*, 645−652.

and the rapid and irreversible interaction of **2d** with H_2O_2 suggest that the system may bear a strong similarity with dinuclear carboxylato-bridged catalase enzymes. Furthermore the formation of high-valent species is at most transient, i.e., during transfer of oxygen to the substrate (or hydrogen abstraction in the case of C−H activation). Indeed several aspects of the catalytic system show remarkable analogy with the manganese catalase[13] enzymes, such as the importance of the carboxylato ligand and the exchange of aqua and aquo ligands with H_2O_2.

It is clear that neither **2a**, **2c,** nor **2d** can effect direct oxygen transfer as all three complexes show full stability in the presence of cyclooctene. However, in the present system it is improbable that the dinuclear complex "splits" to form two mononuclear complexes prior to interaction with H_2O_2. The stability of the complex throughout the reaction and the deactivation of the catalyst observed upon loss of a carboxylato ligand provide credence to this conclusion (Figure S10).

The very transient nature of the "H_2O_2-activated" complex, i.e., the formation of **2d** from **2a**, is rate determining with subsequent reaction of the active species with the alkene being very fast, and the absence of distinct spectroscopic features requires that indirect methods be employed to gain information as to the species nature. ^{18}O isotopic labeling of both H_2O and H_2O_2 provides a powerful probe in this regard as has been demonstarted in the recent work of Que and others on iron-based systems.[8,21] Although it is clear that only one of the oxygen atoms incorporated into the *cis*-diol product originates from H_2O_2 and the other oxygen atom from H_2O, the situation is less clear for the epoxide products, where both H_2O_2 and H_2O provide the oxygen atom. The dependence of ^{18}O incorporation into the epoxide from $H_2{}^{18}O$ on the specific acid employed is as striking as is the relative insensitivity of the 1:1 oxygen incorporation into the *cis*-diol from H_2O and H_2O_2. However, for the epoxide there is a correlation between the selectivity of the catalyst/carboxylic acid system toward the *cis*-diol/epoxide ratio and the incorporation of oxygen into the epoxide from H_2O. The incorporation of oxygen from water into the epoxide product ranges from 18% for the 2,6-dichlorobenzoate complex (*cis*-diol/epoxide ratio 7) to 13.4% for the 2,4-dichlorobenzoic acid complex (*cis*-diol/epoxide ratio 2.7) and to 3.4% for the salicylic acid (*cis*-diol/epoxide ratio 0.7). Hence, the more electrophillic the Mn−OH group of the Mn(OOH)−Mn(OH) species is the higher the *cis*-diol ratio will be. Furthermore, for the more electron withdrawing acid CCl_3CO_2H, although the selectivity toward *cis*-diol formation is lower than that observed for 2,6-dichlorobenzoic acid, the incorporation of oxygen from water into the epoxide product is much higher (33%). In the absence of added carboxylic acid, more oxygen from the H_2O_2 is incorporated into both the *cis*-diol and epoxide products, with a significant amount of *cis*-diol showing both oxygen atoms originating from H_2O_2. This observation can be rationalized by considering that the rate of exchange of Mn−OH with H_2O is slower in the absence of an excess of carboxylic acid.

Scheme 5. Possible H_2O_2-Activated Species and Observed Oxygen Incorporation from H_2O_2 and H_2O in *cis*-Diol and Epoxide Products[a]

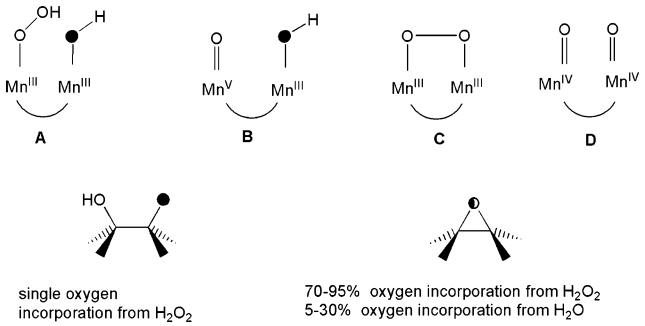

[a] Key: (●) oxygen originating from H_2O.

Several possible dinuclear structures for the "H_2O_2-activated" complex are depicted in Scheme 5. Coordination of H_2O_2 to the manganese center can form either a η^1-O−OH (species A) or Mn−O−O−Mn (species C).

In the case of species A, the homolysis of the O−O bond to form OH* radicals is highly unlikely as the involvement of hydroxyl radicals in the catalytic oxidation has been excluded experimentally.[11] The ability to engage in oxidation of alkanes and alcohols[11] would suggest that a high-valent (e.g., $Mn^V{=}O$)[60] species is involved; however, although heterolysis of the O−O bond in species A would yield a $Mn^{III}Mn^V$ species (B), such a species can exist only transiently before intramolecular electron transfer takes place to form a $(Mn^{IV}{=}O)_2$ species (D).[61]

For species C, direct reaction with the substrate is unlikely as this would result in both oxygens of the dihydrogen peroxide being incorporated into the *cis*-diol product and 100% incorporation into the epoxide. Homolysis of the O−O bond, however, would lead to the formation of the $Mn^{IV}{}_2$ species D, and although exchange of one of the oxygen atoms with water would rationalize the ^{18}O incorporation into the products, a fast exchange of only one of the oxygen atoms with water is required with the remaining oxygen from the dihydrogen peroxide being kinetically inert to exchange. For a symmetric species such as D, such behavior is highly unlikely. The incorporation of oxygen from water into the epoxide would demand that slow exchange takes place as the degree of incorporation is not statistical. Indeed the incorporation of oxygen from water is highly dependent on the nature of the carboxylate employed while for the *cis*-diol product the ratio appears to be dependent, albeit only moderately, on the rate of Mn−OH exchange with water.

It is therefore, in our view, a reasonable assumption that the reaction of H_2O_2 with **2d** leads, initially, to the formation of a $Mn^{III}(O{-}OH)Mn^{III}(OH)$ species, i.e., A. The Mn^{III} center

(60) (a) Adam, W.; Roschmann, K. J.; Saha-Moller, C. R.; Seebach, D. *J. Am. Chem. Soc.* **2002**, *124*, 5068−5073. (b) Meunier, B.; Guilmet, E.; De Carvalho, M.; Poilblanc, R. *J. Am. Chem. Soc.* **2000**, *122*, 2675.

(61) As noted by the reviewers, a μ-oxido-bridged dinuclear iron(IV) oxo complex has been proposed as an active species in the epoxidation and cis-dihydroxylation of alkenes by the following: Kodera, M.; Itoh, M.; Kano, K.; Funabiki, T.; Reglier, M. *Angew. Chem., Int. Ed.* **2005**, *44*, 7104−7106. The rate of exchange of oxygen atoms with water in this species is noted to be fast and results in scrambling of the oxygen atoms derived from homolytic cleavage of the Fe−O−O−Fe bond of a species analogous to species C in Scheme 5.

Scheme 6. Rationalization of H_2O_2 Activation by Dinuclear Manganese Bis(carboxylato)-Bridged Complexes Coordinated to H_2O_2[a]

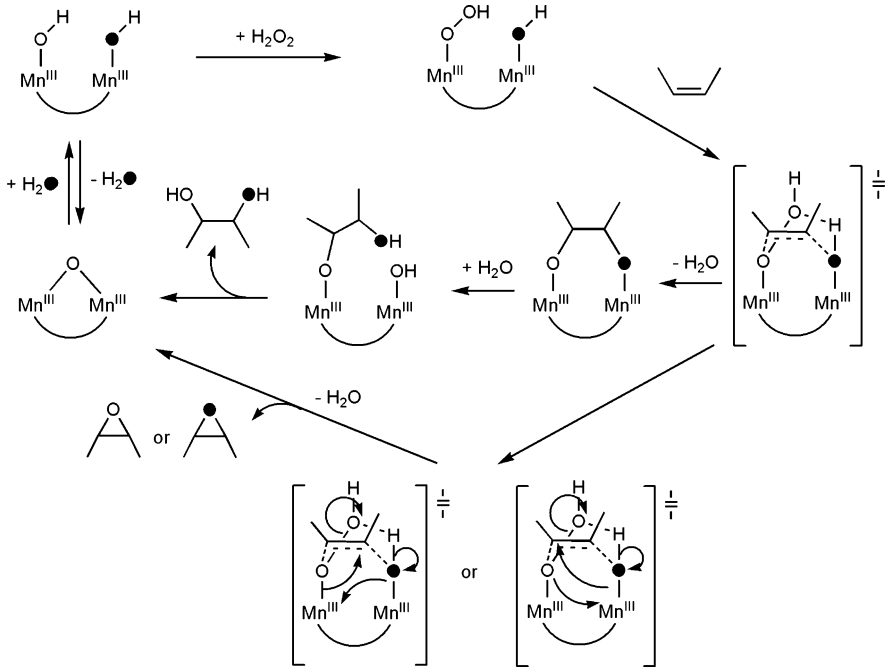

[a] Key: (●) oxygen originating from H_2O.

polarizes the O−O bond to a much greater extent than in a corresponding Mn^{II}−(O−OH) species would (Scheme 6). Such polarization and hence reactivity is facilitated by electron-deficient ligands such as $CCl_3CO_2^-$. Hence the catalyst is expected to be electrophilic in nature, as is observed experimentally. The polarization of the O−O bond is reminiscent of the reductive step of the manganese catalase cycle where the O−OH bond is cleaved by transfer of a proton to the terminal oxygen (i.e., $O-OH_2$).[62] The proton required is available proximally in the present model from the neighboring Mn−OH unit. The more electron withdrawing the carboxylic acid, the greater the acidity of this Mn−OH group will be and hence the more reactive the system.

A mechanism in which a high-valent manganese center is present as a transient intermediate is proposed in Scheme 6. From our earlier studies, we have demonstrated that the oxygen transfer is a concerted process and hence the transfer of both oxygen atoms, one from the solvent and one from H_2O_2, should occur in a single step; i.e., for cis-dihydoxylation and epoxidation both C−O bonds form simultaneously.[11] This mechanism proposes that the oxygen atom of the −OOH ligand, which binds to the manganese center, and to a lesser extent the oxygen atom of the −OH ligand on the adjacent manganese site engage in an electrophilic interaction with the substrate to form the transition state.[63] It is at this point that the differentiation in mechanisms between *cis*-diol formation and epoxidation would be expected to take place. Loss of H_2O, coupled with formation of a Mn−O−Mn bond will result in re-formation of, e.g., **2a** with formation of the epoxide product. This step favors the transfer of the oxygen atom of the Mn−O−O−H unit to the alkene, but with more electron withdrawing carboxylato ligands, the Mn−O−H oxygen can compete with this process. Such a mechanism is in full agreement with ^{18}O-labeling studies for the epoxide product.

For the *cis*-diol product, the loss of H_2O from the transition state is not coupled to formation of an Mn−O−Mn bridge. Instead the *cis*-diol remains bound via both oxygens and must be displaced subsequently by H_2O before reentering the catalytic cycle either as, e.g., **2a** or **2d**. Hence, it would be expected that μ-carboxylato ligands, which inhibit formation of μ-oxido-bridged complexes such as **2a**, should also inhibit the formation of epoxide in favor of *cis*-diol. It is observed empirically that steric hindrance is the most important factor in determining selectivity with more sterically hindered systems favoring cis-dihydroxylation. It would be expected, and it is indeed the case, that incorporation of one oxygen atom from H_2O_2 and one from H_2O into the *cis*-diol product would occur.

Conclusions and Perspectives. Over the past decade considerable successes in enhancing the activity of **1** toward catalytic oxidative transformations were achieved most notably through the use of additives.[17,64] Among the various approaches taken, the use of carboxylic acids has proven to be the most effective in both suppression of the wasteful

(62) Whittaker, M. M.; Barynin, V. V.; Antnyuk, S. V.; Whittaker, J. W. *Biochemistry* **1999**, *38*, 9126−9136.

(63) This mechanism is similar but opposite to the mechanism proposed for a related manganese mononuclear catalyst in which the noncoordinated oxygen atom of the Mn(═O)−O−OH species is activated for oxygen transfer. See: Busch and co-workers.[58b] The approach of the alkene porposed in this work is reminiscent of that proposed by Que and co-workers for a mononuclear Fe(IV)(═O)OH species. See: Bassan, A.; Blomberg, M. R. A.; Siegbahn, P. E. M.; Que, L., Jr. *Angew. Chem., Int. Ed.* **2005**, *44*, 2939−2941.

(64) (a) Woitiski, C. B.; Kozlov, Y. N.; Mandelli, D.; Nizova, G. V.; Schuchardt, U.; Shul'pin, G. B. *J. Mol. Catal., A: Chem.* **2004**, *222*, 103−119 and references therein. (b) Liu, B.; Chen, Y.; Yu, C-Z.; Shen, Z-W. *Chin. J. Chem.* **2003**, *21*, 833−838. (c) Ryu, J. Y.; Kim, S. O.; Nam, W.; Heo, S.; Kim, J. *Bull. Korean Chem. Soc.* **2003**, *24*, 1835−1837.

disproportionation of H_2O_2 and in controlling the activity and selectivity of the catalytic system.[11] In this study, we have demonstrated that carboxylic acids play more than a single role in the enhancement of the catalytic properties of **1**, i.e., as a proton source to facilitate reduction of **1** (by H_2O_2), as a bridging ligand, and in stabilizing the catalytically active bis(μ-carboxylato)$-Mn^{III}_2$ complexes formed after the initial lag period.

It is in acting as a ligand, however, that the carboxylate can exert control over both the activity and selectivity of the catalytically active species. Although a clear relationship between activity and the electron deficiency of the carboxylic acid is apparent, with activity increasing with increased electron-withdrawing character of the carboxylate (i.e., **2a** is more active than **3**), an additional factor which should be considered is the propensity to form species such as **2d**. Overall, carboxylate ligands, which promote formation of such species, show higher activity compared with electronically equivalent carboxylate ligands. With regard to selectivity, steric factors appear to be dominant, with increasing steric hindrance, at the 2,6-positions of the benzoic acid, favoring cis-dihydroxylation over epoxidation.

Understanding the mode of action of promoting agents in catalysis is key to the development of a rational approach to tuning of both the activity and selectivity of the system in question. In this study, we have demonstrated that through a combination of spectroscopic, electrochemical, and catalytic investigations a detailed mechanistic insight into the catalytic system can be deduced. The results obtained highlight the crucial importance of considering both the bulk solvent properties and molecular interactions in understanding catalytic processes. Furthermore, the identification of a dinuclear carboxylato bridged complex as being responsible for catalysis requires that the preference for proposing high-valent manganese oxido species as the active agent in manganese−tmtacn-based catalysis may need to be reconsidered. The model proposed in this contribution provides, in our view, a solid basis for future computational studies and indeed may provide a useful model system for the related bioinorganic dinuclear manganese centers found in catalase enzymes.

Acknowledgment. We thank Ms. T. D. Tiemersma-Wegman, Mr. C. Smit, Ms. A. van Dam, Dr. A. P. Bruins, and Mr. A. Kiewiet for assistance with GC and ESI-MS analysis and the Dutch Economy, Ecology, Technology (Grant EETK01106) program for financial support. We especially thank Prof. Jan Reedijk and Dr. J. Gerard Roelfes for many discussions and their suggestions.

Supporting Information Available: Analytical and experimental data for **2c** and **4**−**16** and mass and UV−vis and EPR spectral data (PDF). This material is available free of charge via the Internet at http://pubs.acs.org.

IC7003613